Molecular Biology of the Cell
Vol. 19, 4454–4468, October 2008

Swf1p, a Member of the DHHC-CRD Family of Palmitoyltransferases, Regulates the Actin Cytoskeleton and Polarized Secretion Independently of Its DHHC Motif

Shubha A. Dighe* and Keith G. Kozminski*†

*Department of Biology, University of Virginia, Charlottesville, VA 22904; and †Department of Cell Biology, University of Virginia School of Medicine, Charlottesville, VA 22904

Submitted March 10, 2008; Revised July 11, 2008; Accepted August 6, 2008
Monitoring Editor: David G. Drubin

Rho and Rab family GTPases play a key role in cytoskeletal organization and vesicular trafficking, but the exact mechanisms by which these GTPases regulate polarized cell growth are incompletely understood. A previous screen for genes that interact with *CDC42*, which encodes a Rho GTPase, found *SWF1/PSL10*. Here, we show Swf1p, a member of the DHHC-CRD family of palmitoyltransferases, localizes to actin cables and cortical actin patches in *Saccharomyces cerevisiae*. Deletion of *SWF1* results in misorganization of the actin cytoskeleton and decreased stability of actin filaments in vivo. Cdc42p localization depends upon Swf1p primarily after bud emergence. Importantly, we revealed that the actin regulating activity of Swf1p is independent of its DHHC motif. A *swf1* mutant, in which alanine substituted for the cysteine required for the palmitoylation activity of DHHC-CRD proteins, displayed wild-type actin organization and Cdc42p localization. Bgl2p-marked exocytosis was found wild type in this mutant, although invertase secretion was impaired. These data indicate Swf1p has at least two distinct functions, one of which regulates actin organization and Bgl2p-marked secretion. This report is the first to link the function of a DHHC-CRD protein to Cdc42p and the regulation of the actin cytoskeleton.

INTRODUCTION

Polarized secretion supported by an asymmetrically organized actin cytoskeleton promotes polarized morphogenesis in many cell types. Recent studies showed that Cdc42p, a small GTPase of the Rho family with multiple distinct functions, is essential for the proper polarization of the actin cytoskeleton and secretory apparatus (reviewed in Nelson, 2003; Etienne-Manneville, 2004; Van Aelst and Cline, 2004; Park and Bi, 2007). For example, in mouse hippocampal neurons, knockout of Cdc42 leads to organizational defects in the actin cytoskeleton (Garvalov *et al*., 2007), whereas, expression of dominant Cdc42 alleles lead to a decrease in the polarized distribution of actin and a specific population of exocytotic vesicles marked with tetanus neurotoxin insensitive-vesicle–associated membrane protein (Alberts *et al*., 2006). Cdc42-dependent defects in exocytosis are not always correlated with defects in the actin cytoskeleton. Expression of dominant-negative Cdc42 in Madin-Darby canine kidney cells, for example, inhibits vesicle trafficking to the basolateral membrane without apparent effect on the actin cytoskeleton (Kroschewski *et al*., 1999). In *Saccharomyces cerevisiae*, alleles of *cdc42* revealed that Cdc42p is necessary for both the polarization of the actin cytoskeleton and the exocyst complex at sites of polarized growth, i.e., the bud tip (Adamo *et al*., 2001; Zhang *et al*., 2001; Roumanie *et al*., 2005). Even with a steady advance toward understanding the mechanics of Cdc42p-dependent cell polarization in recent years, especially the functional links that coordinate the organization and dynamics of the actin cytoskeleton with vesicle trafficking, many of the genes that promote *CDC42*-dependent cell polarization remain unidentified. For this reason, several genetic screens were undertaken to identify genes that promote *CDC42*-dependent cell polarization in *S. cerevisiae* (Kozminski *et al*., 2003).

SWF1/PSL10/YDR126W (hereafter *SWF1*) was one of 30 *CDC42*-interacting genes identified in *S. cerevisiae* in a synthetic genetic interaction screen for genes involved in cell polarization (Kozminski *et al*., 2003). This gene was also identified previously in three independent genetic screens, each of which implicated Swf1p in a specific cellular process. A screen for genes required for meiotic division and recombination identified *SWF1* as important for *s*pore *w*all *f*ormation (Enyenihi and Saunders, 2003). In mitotic cells, in a screen based on the missorting of carboxypeptidase Y, *SWF1* was found involved in vesicle trafficking and sorting to the vacuole (Bonangelino *et al*., 2002). Although seeming dissimilar, all of these cellular processes depend in common upon a functioning actin cytoskeleton (Hill *et al*., 1996; Bonangelino *et al*., 2002; Taxis *et al*., 2006; Isgandarova *et al*., 2007). The idea of a physiological link between *SWF1* function and the actin cytoskeleton is further supported by the identification of *SWF1* as *PSL10* (*p*rofilin *s*ynthetic *l*ethal). Haarer found that deletion of *SWF1* is synthetic lethal with a hypomorphic allele of *PFY1* (Bartels *et al*., 1999), which encodes a potent regulator of the actin cytoskeletal dynamics and organization (Jockusch *et al*., 2007). However, whether *SWF1* regulates the dynamics and organization of the actin cytoskeleton has not been examined.

This article was published online ahead of print in *MBC in Press* (http://www.molbiolcell.org/cgi/doi/10.1091/mbc.E08–03–0252) on August 13, 2008.

Address correspondence to: Keith G. Kozminski (kkoz@virginia.edu).

Abbreviations used: LatA, latrunculin A; PT, palmitoyltransferase.

SWF1 encodes a polypeptide (Swf1p) with five predicted transmembrane domains; it is one of seven proteins in *S. cerevisiae* that contain a DHHC-CRD motif (Putilina *et al*., 1999; Linder and Deschenes, 2003; Politis *et al*., 2005; Mitchell *et al*., 2006). As with many of the >20 DHHC-CRD–containing proteins in mammals (Fukata *et al*., 2004), including Huntingtin interacting protein 14 (Ducker *et al*., 2004), three of the DHHC-CRD proteins in yeast (Erf2p, Pfa3p, and Akr1p) have palmitoyltransferase (PT) activity. Swf1p seems to have PT activity as well (Valdez-Taubas and Pelham, 2005), although in vitro reconstitution of this activity has yet to be demonstrated. Palmitoylation, the result of PT activity, is a posttranslational lipid modification that is essential for the trafficking of signaling molecules such as Ras, and, in the case of mutant huntingtin protein, for the prevention of protein aggregation (see references in Linder and Deschenes, 2007). In budding yeast, Swf1p was shown to palmitoylate the soluble *N*-ethylmaleimide-sensitive factor attachment protein receptor (SNARE) proteins Snc1p, Syn8, and Tlg1p (Valdez-Taubas and Pelham, 2005). Palmitoylation protects the Qc-SNARE Tlg1p from ubiquitin-mediated degradation, suggesting that palmitoylation is one mechanism by which a cell spatially and temporally regulates exocytosis (Valdez-Taubas and Pelham, 2005). One prediction of this model that has not been tested is whether loss of the DHHC motif (i.e., the predicted PT activity) results in a secretory defect, and, if so, whether this secretory defect occurs independently of effects on the actin cytoskeleton. This prediction is tested in this study.

MATERIALS AND METHODS

Strains and Microbial Techniques

Yeast strains and plasmids used in this study are listed in Tables 1 and 2, respectively. *S. cerevisiae* and *Escherichia coli* strains were cultured and transformed as described in Kozminski *et al*. (2003, 2006), unless otherwise noted. Multiple independent transformants or independently derived strains were analyzed in each experiment.

KKY282 and KKY293 were derived from Y3611, by using pKK1469 and pKK1473 as sources of integrating DNA, respectively, following the method that was used to construct KKY281 and KKY 283 (Kozminski *et al*., 2003).

The method of Longtine *et al*. (1998) was used to delete *SWF1* in DDY1102, forming KKY1074. Polymerase chain reaction (PCR) was used to amplify a *kanMX4* disruption cassette with Accuzyme (Bioline, Randolph, MA) from template pML1 with the primers oSD2 (CTCTTTAGGAAATTCGTAGCTATCAACAAAGGTAGTGTCATTGTATATATACTTCCGCCCGGATCCCCGGGTTAATTAA) and oKK144 (AATAAACCGCTTGTATAATGAATTTGTTCGACATTTGCGGTTAGAATCTATGGCGGTGAGGAATTCGAGCTCGTTTAAAC; *SWF1* flanking sequence underlined). The same method was used to introduce a green fluorescent protein (GFP) tag at the C terminus of Swf1p in DDY1102, forming KKY1104. PCR was used to amplify *GFP-kanMX* from template pML4, by using Accuzyme (Bioline) and primers oKK143 (CGAAATTCCCAATATATATGACAAAGGTACCTTCCTGGCCAATCTCACAGATTTAATACGGATCCCCGGGTTAATTAA; *SWF1* flanking sequence underlined) and oKK144.

Plasmids

To construct a 2μ plasmid containing *SWF1* (pKK1585), the region of chromosome IV between base pairs 702754 and 704475 was amplified from KKY283 genomic DNA with BioXact DNA polymerase (Bioline) by using the primers oKK172 (GACTAAGCTTCATTCGCTCATCCTTAAAC; HindIII site underlined) and oKK173 (CTGATCTAGAGTAATATACAATTATCTTACGTAG; XbaI site underlined), and subcloned into the HindIII and XbaI sites of YEplac195. To verify the fidelity of amplification, the subcloned PCR fragment was sequenced. To construct a *CEN* plasmid containing *SWF1* (pKK1586), a HindIII-XbaI fragment from pKK1585 was subcloned into the HindIII and XbaI sites of YCplac33.

To construct pKK1872 (*GST-SWF1-C*), the coding sequence for the nonconserved C terminus (amino acids 235–336) of Swf1p was amplified by PCR from pKK1586 by using the primers oKK170 (GACCAAGCTTCTATATTAAATCTGTGAGATTGGC; HindIII site underlined) and oKK182 (CTGAGGATCCGCCATTGTAAAGGAGGGAATG; BamHI site underlined) and subcloned into the BamHI and HindIII sites of pKK1871. To verify the fidelity of amplification, the subcloned PCR fragment was sequenced. To construct pKK1871 (*GST-SWF1*), the coding sequence of *SWF1* was amplified by PCR from DDY1102 genomic DNA using primers oKK169 (ACGCGGATCCATGTCATGGAATCTACTATTTGTG; BamHI site underlined) and oKK170 and subcloned into the BamH1 and HindIII sites of pKK1516. To construct pKK1516, the coding sequence of *cdc42-118* was amplified by PCR from pAC129 by using primers oKK18 (GCGCGGGATCCATGCAAACGCTAAAGTGTGTTGTTG; BamHI site underlined) and oKK24 (GCGCGCAAGCTTCTACAAAATTGTACATTTTTTACTTTTC; HindIII site underlined) and subcloned into the BamHI and HindIII sites of pKK661.

The QuikChange site-directed mutagenesis kit (Stratagene, La Jolla, CA) was used to construct pKK1873 (*swf1-DHHA*), in which the codon for cysteine 164 was mutagenized to that of alanine. This PCR-based approach used pKK1586 as a template and primers oKK179 (GTCGCCGACCATCATGCCATCTGGATAAATAAC) and oKK180 (GTTATTTATCCAGATGGCATGATGGTCGGCGAC).

Removing a NotI-NotI *LEU2*-containing fragment from pAC183 and pAC329 and replacing it with a NotI-Not1 *natMX*-containing fragment constructed pKK1469 and pKK1473, respectively. The *natMX* fragment was generated by PCR as described in Kozminski *et al*. (2003).

α Factor Release Assay

α Factor (synthesized at the University of Virginia, Charlottesville, VA) was added to log-phase cells (OD_{600} = 0.25), grown in rich medium at 25°C, to a final concentration of 5 μg/ml. After culturing for an additional 90 min, the cells were harvested by centrifugation for 5 min at 1.5 krpm in an IEC clinical centrifuge at room temperature. Each cell pellet was then washed twice with 12.5 ml of rich medium and cultured as described above. After the second wash (t = 0), 0.5 ml of each culture was collected every 10 min and fixed with 4% formaldehyde. Before scoring bud size by phase microscopy, each sample was sonicated briefly.

Exocytosis Assays

Bgl2p secretion was assayed as described in Kozminski *et al*. (2006), following the method of Harsay and Schekman (2007).

To assay for the secretion of invertase (Suc2p), the assay of Bankaitis *et al*. (1989) was used with modification. For each strain assayed, 5 ml of mid-log phase culture (~0.25–0.3 OD_{600}) was pelleted at 600 × *g* for 5 min. The pellet was resuspended in 5 ml of rich medium (5% glucose) and then grown at 25°C for 60 min. To assay NY17 cells at permissive and restrictive temperatures, 10 ml of mid-log phase culture was split equally and processed in parallel, except one culture was preshifted to 37°C for 15 min after 60-min growth at 25°C. Both NY17 cultures were then pelleted as described above and washed with 10 ml of sterile water prewarmed to either 25 or 37°C. After the wash, cells were resuspended in 3 ml of rich medium (0.1% glucose) and incubated at either 25°C or 37°C for 90 min. After this incubation, all cultures, including the NY17 cultures, were harvested as described above. Cells were gently resuspended in 5 ml of ice-cold 10 mM NaN_3/10 mM KF, incubated on ice for 10 min, and then diluted with 5 ml of ice-cold water. The cell suspension was further diluted with ice-cold water if the OD_{600} was >0.7. The cell suspension was centrifuged again as before. Pellets were washed twice with 10 ml of water and then resuspended gently in 1 ml of 0.2 M sodium acetate, pH 4.9. Then, 0.5 ml of each cell suspension was transferred to each of two new microfuge tubes. One tube was maintained on ice, and to the other tube 12 μl of 20% Triton X-100 was added, with gentle mixing followed by one freeze-thaw cycle in a dry ice-ethanol bath. The equivalent of 0.02 OD_{600} units from each sample was assayed for invertase activity following the method of Goldstein and Lampen (1975).

Electron Microscopy

For the analysis of vesicles within yeast, thin sections for transmission electron microscopy were prepared according to the methods of Salminen and Novick (1987) and Wright (2000), with modifications. In brief, 12.5 ml of mid-log phase yeast culture (~6 OD_{600} units), grown in rich medium at 25 or 37°C were rapidly pipetted into an equal volume of 2× fixative (0.2 M sodium cacodylate buffer, pH 6.8, 0.4 M D-sorbitol, 4 mM $MgCl_2$, 4 mM $CaCl_2$, 8% paraformaldehyde, and 6% glutaraldehyde; fixatives from Ted Pella, Redding, CA) and incubated 10 min at room temperature. Cells were then pelleted at 1500*g* for 5 min, resuspended in 25 ml of fixative, and incubated overnight at 4°C. Fixed cells were pelleted at 1500 × *g* for 5 min at room temperature, washed twice with 20 ml of 0.1 M cacodylate buffer, pH 6.8, and then washed twice with 25 ml of 50 mM potassium phosphate buffer, pH 7.5. Cells were then pelleted as described above, resuspended in 1 ml of 50 mM potassium phosphate buffer containing 0.25 mg/ml Zymolyase 100T (Seikagaku, Tokyo, Japan), and incubated at 30°C for 45 min. Fixed spheroplasts were then pelleted at 1000 × *g* for 1 min at room temperature and washed thrice with ice-cold 0.1 M cacodylate buffer. After the wash, pelleted spheroplasts were resuspended in 1 ml of ice-cold 1% (vol/vol) osmium tetroxide and 0.8% (wt/vol) potassium ferricyanide in 0.1 M cacodylate buffer, pH 6.8, for 1 h on ice. The spheroplasts were then washed thrice with deionized water, resuspended in aqueous 0.5% uranyl acetate for 30 min at room temperature in the dark, and then washed twice with deionized water. Graded dehydration with ethanol and then acetone preceded embedment

Table 1. S. cerevisiae strains used in this study

Strain	Relevant genotype	Source
DDY1102 (alias KKY49)	*MAT***a**/*MATα SWF1/SWF1 ura3-52/ura3-52 his3Δ200/his3Δ200 leu2-3,112/leu2-3,112 ADE2/ade2-1 lys2-801/LYS2*	Kozminski *et al*. (2000)
KKY281	*MATα CDC42:natMX can1Δ::MFA1pr-HIS3-MFα1pr-LEU2 his3Δ1 leu2Δ0 ura3Δ0 lys2Δ0*	Kozminski *et al*. (2003)
KKY282	*MATα cdc42-101:natMX can1Δ::MFA1pr-HIS3-MFα1pr-LEU2 his3Δ1 leu2Δ0 ura3Δ0 lys2Δ0*	This study[a]
KKY283	*MATα cdc42-118:natMX can1Δ::MFA1pr-HIS3-MFα1pr-LEU2 his3Δ1 leu2Δ0 ura3Δ0 lys2Δ0*	Kozminski *et al*. (2003)
KKY293	*MATα cdc42-129:natMX can1Δ::MFA1pr-HIS3-MFα1pr-LEU2 his3Δ1 leu2Δ0 ura3Δ0 lys2Δ0*	This study[a]
KKY1060	*MAT***a**/*MATα swf1Δ::kanMX4/swf1Δ::kanMX4 ura3-52/ura3-52 his3Δ200/his3Δ200 leu2-3,112/leu2-3,112 ADE2/ade2-1 lys2-801/lys2-801*	KKY1063 × KKY1065
KKY1062	*MAT***a**/*MATα SWF1/swf1Δ::kanMX4 ura3-52/ura3-52 his3Δ200/his3Δ200 leu2-3,112/leu2-3,112 ADE2/ade2-1 lys2-801/lys2-801*	KKY1064 × KKY1065
KKY1063	*MATα swf1Δ::kanMX4 ura3-52 his3Δ200 leu2-3,112 lys2-801*	Meiotic product of KKY1074
KKY1064	*MATα ura3-52 his3Δ200 leu2-3,112 lys2-801*	Meiotic product of KKY1074
KKY1065	*MAT***a** *swf1Δ::kanMX4 ura3-52 his3Δ200 leu2-3,112 ade2-1 lys2-801*	Meiotic product of KKY1074
KKY1067	*MAT***a** *swf1Δ::kanMX4 CDC42:natMX his3Δ1 leu2Δ0 ura3Δ0 lys2Δ0 can1Δ::MFA1pr-HIS3-MFα1pr-LEU2*	Meiotic product of KKY1145
KKY1068	*MAT***a** *swf1Δ::kanMX4 cdc42-118:natMX his3Δ1 leu2Δ0 ura3Δ0 lys2Δ0 can1Δ::MFA1pr-HIS3-MFα1pr-LEU2*	Meiotic product of KKY1144
KKY1069	*MAT***a**/*MATα swf1Δ::kanMX4/SWF1 CDC42/cdc42-129:natMX his3Δ1/his3Δ1 leu2Δ0/leu2Δ0 ura3Δ0/ura3Δ0 lys2Δ0/LYS2 CAN1/can1Δ::MFA1pr-HIS3-MFα1pr-LEU2 met15Δ0/MET15*	KKY293 × 1-7-11
KKY1070	*MAT***a** *swf1Δ::kanMX4 cdc42-101:natMX his3Δ1 leu2Δ0 ura3Δ0 lys2Δ0 can1Δ::MFA1pr-HIS3-MFα1pr-LEU2*	Meiotic product of KKY1143
KKY1074	*MAT***a**/*MATα swf1Δ::kanMX4/SWF1 his3Δ200/his3Δ200 leu2-3,112/leu2-3,112 ura3-52/ura3-52 ADE2/ade2-1 lys2-801/LYS2*	This study[a]
KKY1084	KKY1064 [pKK1586, YCplac33(*SWF1*)]	This study[b]
KKY1085	KKY1064 [pKK1873, YCplac33(*swf1-DHHA*)]	This study[b]
KKY1086	KKY1063 [pKK1586,YCplac33(*SWF1*)]	This study[b]
KKY1087	KKY1063 [pKK1873, YCplac33(*swf1-DHHA*)]	This study[b]
KKY1088	*MAT***a** *pfy1-4:LEU2 ura3-52 his3Δ200 leu2-3,112 lys2-801*	This study[c]
KKY1090	*MATα swf1Δ::kanMX4 ura3-52 his3Δ200 leu2-3,112 lys2-801*	This study[d]
KKY1104	*MAT***a**/*MATα SWF1-GFP:kanMX4/SWF1 his3Δ200/his3Δ200 ura3-52/ura3-52 leu2-3,112/leu2-3,112 ADE2/ade2-1 lys2-801/LYS2*	This study[a]
KKY1120	MAT**a** */MATα his3Δ1/his3Δ1 leu2Δ0/leu2Δ0 LYS2/lys2Δ0 met15Δ0/MET15*	BY4741 × BY4742
KKY1134	*MAT***a** *swf1Δ::kanMX4 cdc42-101:natMX his3Δ1 leu2Δ0 ura3Δ0 lys2Δ0 can1Δ::MFA1pr-HIS3-MFα1pr-LEU2* [YCplac33]	This study[e]
KKY1135	*MAT***a** *swf1Δ::kanMX4 cdc42-101:natMX his3Δ1 leu2Δ0 ura3Δ0 lys2Δ0 can1Δ::MFA1pr-HIS3-MFα1pr-LEU2* [pKK1586,YCplac33(*SWF1*)]	This study[e]
KKY1136	*MAT***a** *swf1Δ::kanMX4 cdc42-101:natMX his3Δ1 leu2Δ0 ura3Δ0 lys2Δ0 can1Δ::MFA1pr-HIS3-MFα1pr-LEU2* [pKK1873, YCplac33(*swf1-DHHA*)]	This study[e]
KKY1137	KKY1068 [YCplac33]	This study[b]
KKY1138	KKY1068 [pKK1586,YCplac33(*SWF1*)]	This study[b]
KKY1139	KKY1068 [pKK1873, YCplac33(*swf1-DHHA*)]	This study[b]
KKY1140	*MAT***a** *swf1Δ::kanMX4 cdc42-129:natMX his3Δ1 leu2Δ0 ura3Δ0 lys2Δ0 can1Δ::MFA1pr-HIS3-MFα1pr-LEU* [pKK1586,YCplac33(*SWF1*)]	This study[f]
KKY1141	KKY1069 [YCplac33]	This study[b]
KKY1142	KKY1069 [pKK1873, YCplac33(*swf1-DHHA*)]	This study[b]
KKY1143	*MAT***a**/*MATα swf1Δ::kanMX4/SWF1 CDC42/cdc42-101:natMX his3Δ1/his3Δ1 leu2Δ0/leu2Δ0 ura3Δ0/ura3Δ0 lys2Δ0/lys2Δ0 CAN1/can1Δ::MFA1pr-HIS3-MFα1pr-LEU2 met15Δ0/MET15*	KKY282 × 1-7-11
KKY1144	*MAT***a**/*MATα swf1Δ::kanMX4/SWF1 CDC42/cdc42-118:natMX his3 Δ1/his3Δ1 leu2Δ0/leu2Δ0 ura3Δ0/ura3Δ0 lys2Δ0/lys2Δ0 CAN1/can1Δ::MFA1pr-HIS3-MFα1pr-LEU2 met15Δ0/MET15*	KKY283 × 1-7-11
KKY1145	*MAT***a**/*MATα swf1Δ::kanMX4/SWF1 CDC42/CDC42:natMX his3Δ1/his3Δ1 leu2Δ0/leu2Δ0 ura3Δ0/ura3Δ0 lys2Δ0/lys2Δ0 CAN1/can1Δ::MFA1pr-HIS3-MFα1pr-LEU2 met15Δ0/MET15*	KKY281 × 1-7-11
KKY1146	*MAT***a** *swf1Δ::kanMX4 ura3-52 his3Δ200 leu2-3,112 lys2-801*	Meiotic product of KKY1074
KKY1147	*MAT***a** *ura3-52 his3Δ200 leu2-3,112 lys2-801*	Meiotic product of KKY1074
DDY663	*MATα ura3-52 leu2-3,112 lys2-801*	D. Drubin[g]
DDY664	*MAT***a** *ura3-52 leu2-3,112 lys2-801*	D. Drubin[g]
DDY1300	*MAT***a** *CDC42:LEU2 ura3-52 leu2-3,112 his3Δ200 lys2-801*	Kozminski *et al*. (2000)
DDY1304	*MAT***a** *cdc42-101:LEU2 ura3-52 leu2-3,112 his3Δ200 lys2-801*	Kozminski *et al*. (2000)
DDY1326	*MAT***a** *cdc42-118:LEU2 ura3-52 leu2-3,112 his3Δ200 lys2-801*	Kozminski *et al*. (2000)
DDY1336	*MAT***a** *cdc42-123:LEU2 ura3-52 leu2-3,112 his3Δ200 lys2-801*	Kozminski *et al*., (2000)
DDY1344	*MAT***a** *cdc42-129:LEU2 ura3-52 his3Δ200 leu2-3,112 lys2-801*	Kozminski *et al*. (2000)
DDY2008	*MAT***a** *pfy1-4:LEU2 ura3-52 his3Δ200 leu2-3,112 lys2-801*	Wolven *et al*. (2000)
1-7-11	*MAT***a** *swf1Δ::kanMX4 ura3Δ0 his3Δ1 leu2Δ0 met15Δ0*	Winzeler *et al*. (1999)
BY4741	*MAT***a** *his3Δ1 leu2Δ0 ura3Δ0 met15Δ0*	Brachmann *et al*. (1998)
BY4742	*MATα his3Δ1 leu2Δ0 ura3Δ0 lys2Δ0*	Brachmann *et al*. (1998)
NY17	*MAT***a** *sec6-4 ura3-52*	Novick *et al*. (1980)
Y3611	*MAT***a**/*MATα can1Δ::MFA1pr-HIS3-MFα1pr-LEU2/CAN1 his3Δ1/his3Δ1 leu2Δ0/leu2Δ0 ura3Δ0/ura3Δ0 met15Δ0/MET15 lys2Δ0/LYS2*	Kozminski *et al*. (2003)

[a] See *Materials and Methods*.

[b] By transformation with indicated plasmid.

[c] Progeny of backcross of DDY2008 with DDY663.

[d] Progeny of backcross of KKY1063 with DDY663.

[e] Meiotic product of KKY1143 transformed with indicated plasmid.

[f] Meiotic product of KKY1069 transformed with indicated plasmid.

[g] University of California at Berkeley.

Table 2. Plasmids used in this study

Plasmid	Relevant genotype	Source
pAC129	pALTER-1(*cdc42–118*)	Kozminski *et al*. (2000)
pAC183	pRS305(*cdc42–101:LEU2*)[a]	Kozminski *et al*. (2000)
pAC329	pRS305(*cdc42–129:LEU2*)[a]	Kozminski *et al*. (2000)
pGAT2	pBAT(*GST*)	Peränen *et al*. (1996)
pML1	pFA6a-kanMX6	Longtine *et al*. (1998)
pML4	pFA6a-GFP(S65T)-kanMX6	Longtine *et al*. (1998)
YCplac33	*CEN URA3*	Gietz and Sugino (1988)
YEplac195	2 μ *URA3*	Gietz and Sugino (1988)
pKK661	pGAT2(*CDC42*)	Kozminski *et al*. (2003)
pKK1469	pRS305(*cdc42–101:natMX*)[a]	This study
pKK1473	pRS305(*cdc42–129:natMX*)[a]	This study
pKK1516	pGAT2(*GST-cdc42–118*)	This study
pKK1585	YEplac195(*SWF1*)	This study
pKK1586	YCplac33(*SWF1*)	This study
pKK1871	pGAT2(*GST-SWF1*)	This study
pKK1872	pGAT2(*GST-SWF1-C*)	This study
pKK1873	YCplac33(*swf1-DHHA*)	This study

[a] Modified pRS305 vector lacking *LEU2*. Alias of this vector is pKK294 (Kozminski *et al*., 2000).

with Spurr's resin. Silver/gold thin sections were cut with a diamond knife and stained with lead citrate (Venable and Coggeshall, 1965) for 5 min, 3% uranyl acetate in 50% acetone for 15 min, and lead citrate again for 5 min. Stained sections were examined on a JEOL 100CXII electron microscope (JEOL, Tokyo, Japan) equipped with a SIA L-3C digital camera (Scientific Instruments and Applications, Atlanta, GA).

Glutathione Transferase (GST)-Swf1-C Expression and Purification

GST-Swf1-C was purified from BL21(DE3) *E. coli* transformed with pKK1872 after an overnight induction at 25°C with 0.1 mM isopropyl β-D-thiogalactoside. All subsequent procedures were completed at 4°C. Bacteria were harvested from a 1-l culture at 4000 rpm (20 min; Beckman J6 rotor). The pellet was resuspended in 40 ml of ice-cold lysis buffer (50 mM Tris-Cl, pH 8.0, 1 mM EDTA, 1 mM dithiothreitol [DTT], 250 mM NaCl, 1 mM phenylmethylsulfonyl fluoride [PMSF], and 0.5 μg/ml each of leupeptin, aprotinin, pepstatin A, chymostatin, and antipain). Bacteria were then lysed on ice with sonication. Lysate was centrifuged at 35,000 rpm for 45 min in a Beckman Ti45 rotor. The supernatant was recovered and nutated with 2 ml of glutathione-Sepharose beads (GE Healthcare, Little Chalfont, Buckinghamshire, United Kingdom), prewashed in lysis buffer, for 20 min. After this incubation, the bead suspension was poured into a column and successively washed with 25 ml of wash buffer [50 mM Tris-Cl, pH 8.0, 1 mM EDTA, 0.5 mM EGTA, 1 mM DTT, 200 mM NaCl, 5% (vol/vol) glycerol, and 1 mM PMSF], 250 ml of wash buffer with 1% Triton X-100, 250 ml of wash buffer with 400 mM NaCl, 250 ml of wash buffer with 1% betaine and 0.1% Tween 20, and 250 ml of wash buffer. GST-Swf1-C was eluted as 1-ml fractions with elution buffer [50 mM Tris-Cl, pH 8.0, 150 mM NaCl, 1 mM DTT, 0.5 mM EDTA, 0.1 mM EGTA, 5% (vol/vol) glycerol, and 25 mM glutathione] until the absorbance of the eluate at 280 nm reached 0.02. Peak GST-Swf1-C fractions, as determined by absorbance spectroscopy at 280 nm and SDS-polyacrylamide gel electrophoresis (PAGE), were pooled (~4 ml total volume) and twice dialyzed against 1.5 l of phosphate-buffered saline (PBS) containing 0.1 mM DTT and 10% (vol/vol) glycerol. Final protein concentration was determined by UV absorbance at 280 nm or by Bradford assay (Bio-Rad, Hercules, CA), by using bovine serum albumin (BSA) as a standard.

Swf1p Antibody Production and Purification

Because thrombin cleavage of the GST-Swf1-C fusion protein resulted in complete degradation of the Swf1 fragment, uncleaved GST-Swf1-C was used as an immunogen. Covance Research Products (Denver, PA) performed all inoculations and bleeds. We brought 250 μg of GST-Swf1-C to 0.5 ml with PBS and mixed with 0.5 ml of Freund's complete adjuvant before subcutaneous injection into New Zealand White rabbits. Booster injections containing 125 μg of GST-Swf1-C and Freund's incomplete adjuvant were administered 3 wk after the initial injection. Bleeds were collected 10 d after each injection and screened for immunoreactivity against Swf1p in whole cell lysates of wild-type yeast (DDY1102). A strain lacking Swf1p (KKY1060) was used as a control. Immunoreactivity was first detected in lysates at week 10. Exsanguination occurred at week 16.

The purification of antibodies against Swf1p proceeded in two steps. First, antibodies against GST were depleted from serum by affinity chromatography, by using a GST column prepared as described in Kozminski *et al*. (2000). Depletion was confirmed by probing dot blots of recombinant GST with crude serum or with the eluate of the GST column. Second, serum depleted of antibodies against GST and diluted 1:50 in Tris-buffered saline containing 1 mg/ml BSA was preabsorbed three times, at room temperature for 2 h each, against nitrocellulose filters containing whole cell lysates of a *swf1*Δ/*swf1*Δ strain KKY1060.

Fluorescence Microscopy

Cells prepared for direct or indirect fluorescence microscopy were observed with epifluorescence on a Nikon E800 microscope equipped with a 100×/1.3 Plan Neofluar objective. Images were captured with an Orca 100ER digital camera (Hamamatsu Photonics, Hamamatsu City, Japan) and Openlab software (Improvision, Lexington, MA). Unless otherwise noted, exposure and contrast enhancement were constant and linear for each image series.

Cells were prepared for indirect immunofluorescence microscopy as described in Kozminski *et al*. (2000, 2006), except when cells were probed with antibody against Tpm1p or Cdc11p. In those cases, methanol and acetone replaced SDS at the permeabilization step per the method of Pringle *et al*. (1989). Polyclonal rabbit antibodies against Swf1p (this study), Cdc42p (Kozminski *et al*., 2000), GFP (Abcam, Cambridge, MA), Tpm1p (Pruyne *et al*., 1998), and Cdc11p (Santa Cruz Biotechnology, Santa Cruz, CA) were used at 1:100, 1:625, 1:1000, 1:50, and 1:300, respectively. Guinea pig polyclonal antibody against yeast actin (Palmgren *et al*., 2001) was used at 1:250. Secondary antibodies goat anti-rabbit Alexa 568-conjugated (Invitrogen, Carlsbad, CA), goat anti-rabbit fluorescein isothiocyanate (FITC)-conjugated (Jackson ImmunoResearch Laboratories, West Grove, PA), and donkey anti-guinea pig rhodamine-conjugated (Jackson ImmunoResearch Laboratories) were used at 1:50 per the manufacturers' instructions.

Actin localization in fixed cells by using rhodamine-conjugated phalloidin (Invitrogen) followed a modified method of Adams and Pringle (1991). One milliliter of mid-log phase yeast culture was fixed for 20 min at room temperature with 5% (vol/vol) formaldehyde. Cells were pelleted in a microfuge for 1 min at 8000 × *g*, washed twice with 1 ml of PBS, and then resuspended in PBS containing 0.1% (vol/vol) Triton X-100 for 4 min at room temperature. Detergent was removed with two additional PBS washes. Pelleted cells were resuspended in 2.2 μM rhodamine-conjugated phalloidin in PBS and incubated 2 h in the dark at room temperature. To remove excess rhodamine-conjugated phalloidin, stained cells were washed three times with 1 ml of PBS containing 0.1% (vol/vol) Triton X-100. After the last wash, cells were resuspended in 10–20 μl of mounting medium. Then, 3–4 μl of stained cell suspension was applied to a slide, after which a coverslip was affixed with nail polish.

The staining of bud scars with Calcofluor White (Fluorescent Brightner 28; Sigma-Aldrich, St. Louis, MO) followed the method of Pringle (1991).

Immunoblotting

Immunoblotting was performed as described in Kozminski *et al*. (2000, 2006). Swf1p was detected with purified anti-Swf1p antibodies diluted 1:1000. Tubulin served as a loading control and was detected with AA2, a mouse monoclonal antibody raised against amino acids 412–430 of bovine brain β-tubulin (gift of A. Frankfurter, University of Virginia), diluted to 130 ng/ml.

Assays of Actin Dynamics

To compare the sensitivity of yeast to latrunculin A (LatA), halo assays were performed. For each strain tested, an overnight culture grown in rich medium was diluted to 0.1 OD_{600} and plated on rich medium. After aspiration of excess culture, plates were dried for 1 h. Each of three different concentrations of LatA (BIOMOL Research Laboratories, Plymouth Meeting, PA), serially diluted with dimethyl sulfoxide, was spotted (10 μl) onto 6-mm concentration disks (B231039; Fisher Scientific, Sparks, MD), which were then placed on the lawn of cells. Plates were incubated at 25° for 2 d. The diameter of the zone of no growth around each disk was measured and used to calculate the relative apparent sensitivity of each strain to LatA following the method of Reneke *et al*. (1988).

To compare the turnover of actin filaments in vivo among different yeast strains, the method of Lappalainen and Drubin (1997) was used. Briefly, log-phase cultures grown in rich medium at 25°C were diluted to 0.4 OD_{600}. LatA was then added to each 0.4-ml culture to 0.4 mM final. At 0, 2, and 6 min post-LatA addition, a 125-μl aliquot of each culture was fixed with 4.4% (vol/vol) paraformaldehyde for 20 min at room temperature. Fixed cells were then stained with 6.6 μM rhodamine-phalloidin (Invitrogen) in methanol and imaged as described above.

Actin Binding Assays

To determine whether the C-terminal domain of Swf1p binds filamentous actin (F-actin), a supernatant depletion assay (Mullins *et al*., 1997) was performed. For 200-μl reactions, rabbit muscle F-actin (kind gift of Dr. D. Schafer, University of Virginia) in MKEI-50 (20 mM imidazole-KOH, pH 7.0, 50 mM

KCl, 2 mM $MgCl_2$, and 1 mM EGTA) was diluted to a final concentration between 15 and 0.15 μM in MKEI-50 containing 0.5× G buffer (2 mM Tris-Cl, pH 8.0, 0.2 mM ATP, 0.2 mM $CaCl_2$, 0.1 mM DTT, and 0.005% NaN_3). Then, 2 μl of GST-Swf1-Cp in PBS containing 10% glycerol and 0.1 mM DTT was mixed into each reaction to give a final fusion protein concentration of 1.5 μM. Reactions were incubated 1 h at room temperature and then ultracentrifuged at 70,000 rpm in a TLA120.1 rotor for 60 min at 4°C. The top 120 μl of supernatant was collected from each reaction and mixed with 40 μl of 4× protein sample buffer (4% SDS, 20% glycerol, 0.2M Tris-Cl, pH 7.0, 4 mM EDTA, 0.16 M DTT, and 0.2 mg/ml bromphenol blue). Equivalent volumes were then analyzed on a 13% SDS-PAGE gel stained with Coomassie Blue.

To determine whether the C-terminal domain of Swf1p binds G-actin, a pyrene–actin assembly assay was performed. For a 200-μl reaction, 16 μM rabbit muscle G-actin (5% pyrene-labeled; kind gift of Dr. D. Schafer) in G buffer was diluted to 4 μM in MKEI-50 containing 0.6× G buffer. Then, 10 μl of GST-Swf1-Cp in PBS containing 10% glycerol and 0.1 mM DTT (or buffer alone) was mixed into the reaction. Fluorescence intensity over time at 25°C was measured immediately using a QuantaMaster fluorometer (Photon Technology International, Birmingham, NJ).

RESULTS

Genetic Analysis Reveals a Functional Relationship between SWF1 and CDC42

We identified *SWF1* in a synthetic genetic array screen for genes that promote polarized cell growth (Kozminski *et al*., 2003). *SWF1* conferred a growth defect when deleted in combination with *cdc42-118^{ts}*, an allele conditionally defective in polarity establishment (Kozminski *et al*., 2000). Of the 30 genes identified in this screen, 20, including *SWF1*, were not previously associated with polarized cell growth. Therefore, this screen associated *SWF1* for the first time with the process of polarized cell growth.

To begin to understand how *SWF1* functions in the process of polarized cell growth, we first examined haploid and diploid strains lacking *SWF1*. We found that haploid cells with a *SWF1* deletion doubled in log phase culture at 25°C at one third to one half the rate measured for congenic wild-type cells. A difference in doubling rate was also observed on solid media, in which haploid *swf1*Δ and homozygous diploid *swf1*Δ/*swf1*Δ cells formed smaller colonies than wild-type cells (Figure 1A). This slower rate of growth was not due a partial block at a specific cell cycle phase, but rather it seemed to be due to a slower rate of bud growth in the mutant cells relative to wild-type cells. Asynchronous cultures of the haploid wild-type and *swf1*Δ strains contained a very similar morphological distribution of cells throughout the cell cycle, as assayed by a visual scoring of bud size (Supplemental Table 1). The only notable difference between these cultures was that the *swf1*Δ culture contained fewer unbudded cells than the wild-type culture, 30 versus 43%, respectively. A similar, but smaller difference, was also observed in asynchronous cultures of the wild-type and homozygous *swf1*Δ/*swf1*Δ diploid cells (Supplemental Table 1). Consistent with a bud growth defect rather than a bud emergence defect, *swf1*Δ and *SWF1* haploid cells initiated bud emergence at approximately the same time after release from α-factor arrest (Supplemental Figure 1). The *swf1*Δ growth phenotype was recessive; a heterozygous (*swf1*Δ/*SWF1*) diploid strain grew at the same rate as a congenic wild-type (*SWF1/SWF1*) strain (Figure 1A). Calcofluor staining did not reveal any defects in bud site selection in the mutant cells (data not shown).

Consistent with the results of the synthetic genetic array screen described above, synthetic sickness was found at 25°C when *swf1*Δ was absent, in haploid cells, in combination with *cdc42-118* (Figure 1B). Mutations that have a synthetic interaction with *cdc42-118* often show the same interaction with *cdc42-101*, an allele that also confers a temperature-conditional polarized growth defect in G1 of the cell cycle. Surprisingly, deletion of *SWF1* suppressed the growth defect of *cdc42-101* at restrictive temperature (Figure 1B). In addition, *swf1*Δ was found synthetic lethal with *cdc42-129*, an allele that inhibits the G2/M switch from apical-to-isotropic bud growth. These synthetic genetic interactions did not seem to be an additive effect. That is, synthetic sickness between *swf1*Δ and temperature-conditional alleles of *CDC42* did not correlate with the restrictive temperature range of the *cdc42* alleles (Figure 1B). Although the molecular basis for the specificity of these genetic interactions is unknown, these results indicated that *SWF1* functions in or in parallel with one or more *CDC42*-dependent pathways that regulate polarized cell growth.

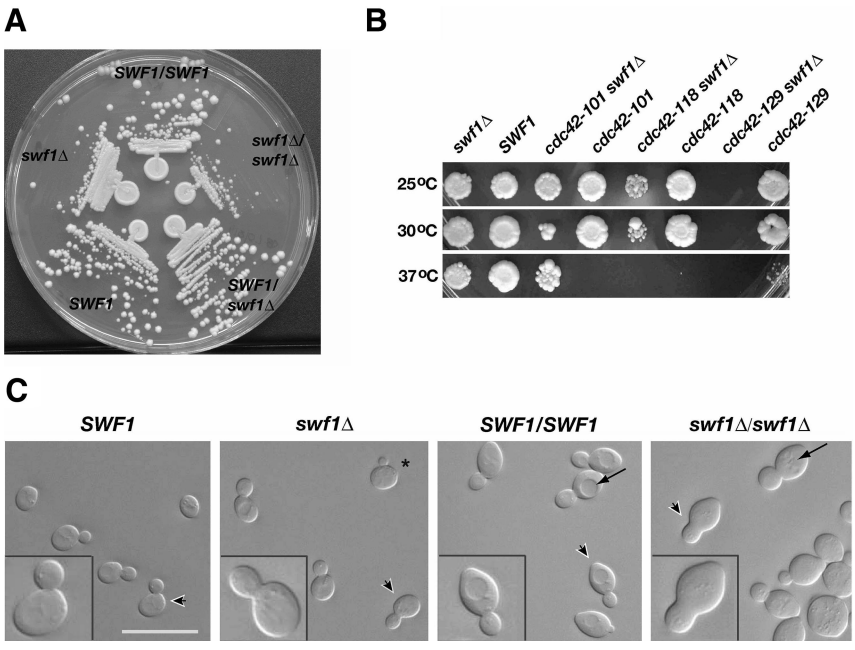

Figure 1. Analyses of the growth, genetic interactions, and morphology of cells lacking *SWF1*. (A) Cells lacking *SWF1* formed smaller colonies than wild-type cells. Wild-type and mutant cells were streaked on rich medium and grown for 2 d at 25°C. Shown clockwise, wild-type diploid (DDY1102), homozygous mutant (KKY 1060), heterozygous mutant (KKY1062), wild-type haploid (KKY1064), and mutant haploid (KKY1063). (B) *swf1*Δ displayed synthetic genetic interaction with *cdc42* alleles defective in distinct processes. Equivalent dilutions of *SWF1*, *swf1*Δ, *cdc42*, and *swf1*Δ *cdc42* strains were plated and grown at 25, 30, and 37°C for 2 d on rich medium. The strains shown (from left to right) are KKY1067, 281, 1070, 282, 1068, 283, and 293. No *swf1*Δ *cdc42-129* cells were plated because these two alleles are lethal in combination. (C) Cells that lacked *SWF1* had an aberrant morphology, most notably a thickening of the mother-bud neck (compare insets). Shown from left to right are differential interference-contrast images of log-phase congenic haploid wild-type (KKY1064) and *swf1*Δ cells (KKY1063) as well as diploid wild-type (DDY1102) and *swf1*Δ/*swf1*Δ cells (KKY1060) grown in rich medium at 25°C. Arrowheads indicate the cells presented in the insets at an enlarged view. Arrows indicate vacuoles. Bar, 10 μm.

SWF1 Is Required for Proper Polarized Cell Growth and Regulates Actin

The genetic interaction found between *SWF1* and *CDC42* and the dependency of SNARE palmitoylation upon Swf1p in vivo (Valdez-Taubas and Pelham, 2005) suggested that *SWF1* is necessary for proper polarized cell growth. Consistent with this prediction, we found that both haploid and diploid cells lacking *SWF1* displayed an aberrant morphology. In comparison with wild-type cells, *swf1*Δ haploid cells seemed rounder (see cell with asterisk in Figure 1C). Diploids homozygous for *swf1*Δ (Figure 1C) but not heterozygous (data not shown) displayed a similar mutant morphology. The aberrant thickening of the neck was especially noticeable in mutant diploid cells, along with fragmentation of the vacuole, which was less apparent in *swf1*Δ haploid cells (Figure 1C).

To determine whether cells lacking *SWF1* are defective in cell polarization, as implied by the genetic interactions between *swf1*Δ and *cdc42-118*^{ts}, we used the cell cycle-dependent organization of the cortical actin cytoskeleton as a readout for cell polarization. In unbudded wild-type cells in late G1, cortical actin patches are concentrated at the incipient bud site. In S and G2 phases of the cell cycle, cortical actin patches are found at the apical tip of small- and medium-sized buds, with actin cables running parallel to the mother-bud axis (Figure 2A, left). This pattern of cytoskeletal organization was significantly different in *swf1*Δ haploid cells (Figure 8A, top right) and *swf1*Δ/*swf1*Δ diploid cells (Figure 2A, right). Actin patches were no longer found polarized at the apical bud tip in mutant cells to the extent found in wild-type cells (Figure 2A). Rather, in *swf1*Δ/*swf1*Δ cells, actin patches were found distributed throughout mother cells and buds, often in greatest concentration at the bud neck. Only 58% of small- and medium-budded mutant cells had properly polarized actin patches, in comparison with 100% of the budded wild-type cells (Figure 2B). In mutant cells, loss of cell polarization was not restricted to one phase of the cell cycle. Only 18% of unbudded *swf1*Δ/*swf1*Δ cells, grown in rich medium, displayed polarization of the cortical actin cytoskeleton, in comparison with 62% of wild-type cells grown under the same conditions (Figure 2B). Consistent with a previous report (Bonangelino *et al*., 2002), actin cables were difficult to observe, if observed at all, in both *swf1*Δ haploid and homozygous diploid mutants (Figures 8A and 2, A and C, respectively). When actin cables were observed in mutant cells, they seemed short and very thin compared with those observed in wild-type cells (Figure 2, A and C). Cables rarely ran the complete length of the mother cell in cells lacking *SWF1*, although they were frequently found to extend from bud site to opposite pole in wild-type cells. These differences were accentuated when cables were visualized independently of actin patches (Figure 2C), by using an antibody against tropomyosin (Tpm1p), an F-actin binding protein that associates exclusively with actin cables (Pruyne *et al*., 1998). These results indicate that *SWF1* is necessary for proper cell polarization and actin organization.

Changes in actin dynamics can cause a misorganization of the actin cytoskeleton (Belmont and Drubin 1998; Belmont *et al*., 1999). To determine whether actin dynamics was altered in vivo in the absence of Swf1p, we assayed a *swf1*Δ strain for sensitivity to the drug LatA. Cells that rapidly turnover F-actin structures are known to be hypersensitive to LatA (Ayscough *et al*., 1997; Lappalainen and Drubin, 1997). Using a halo assay, we found that *swf1*Δ cells are hypersensitive to LatA. The zone of no colony growth around LatA-impreg-

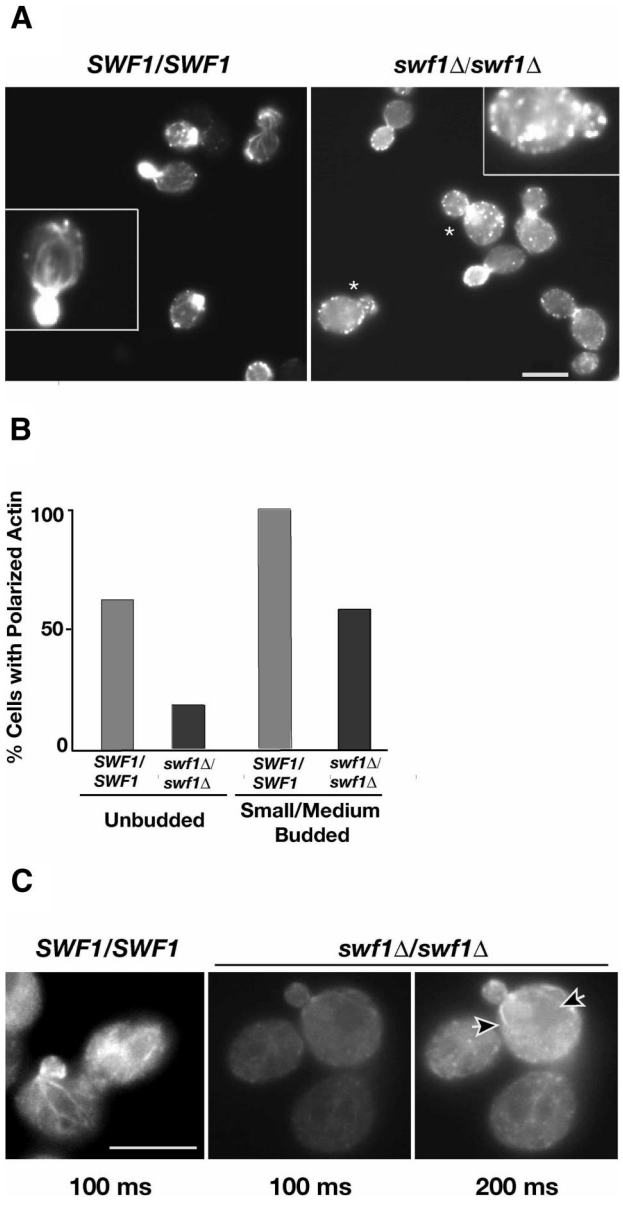

Figure 2. Cell polarization was disrupted in the absence of *SWF1*. (A) Log phase wild-type (DDY1102; left) and homozygous mutant diploid (KKY1060; right) cells, grown in rich medium at 25°C, stained with rhodamine-phalloidin. The inset in the left panel shows a cell with a polarized cortical actin cytoskeleton, and the inset in the right panel shows a cell with a nonpolarized cortical actin cytoskeleton. Polarization of the cortical actin cytoskeleton (actin patches) was absent in many *swf1*Δ/*swf1*Δ cells; examples are marked with asterisk. Bar, 5 μm. (B) Comparison of the number of wild-type and mutant cells with a polarized cortical actin cytoskeleton at different cell cycle phases. The cortical actin cytoskeleton was scored as polarized when cortical actin patches were distributed to one pole of unbudded cells or were distributed to the bud in small- and medium-budded cells. All scored cells had single nucleus as visualized with 4,6-diamidino-2-phenylindole (DAPI). n > 325 scored for each morphological class. The cells quantified were from the same experiment shown in A. (C) Indirect immunofluorescence micrographs of log phase wild-type (DDY1102; left) and homozygous mutant diploid (KKY1060; middle and right) cells, grown in rich medium at 25°C, and probed with anti-tropomyosin (Tpm1p) and goat anti-rabbit-Alexa 568 antibodies. Tpm1-marked actin cables were shorter in *swf1*Δ/*swf1*Δ cells (arrowheads), compared with wild-type, and required twice the image acquisition time to visualize. The middle and right panels are identical, except for the image acquisition time, which is indicated below each panel. Bar, 5 μm.

nated filter disks was of greater diameter on a lawn of *swf1*Δ cells than on a lawn of wild-type cells (Figure 3A). We calculated the relative apparent LatA sensitivity of the *swf1*Δ to be two- to threefold greater than that of wild-type cells. To determine whether actin is indeed rapidly turning over in vivo in the absence of Swf1p, we performed a microscopic LatA sensitivity assay. *swf1*Δ and wild-type cultures were incubated briefly with 400 μM LatA. Aliquots of these cultures were fixed post-LatA addition at 0 min (the time to draw an aliquot and add fixative), 2 min, and 6 min, and then they were processed with rhodamine-phalloidin to visualize F-actin patches by fluorescence microscopy (Figure 3B). Figure 8A shows that in the absence of LatA wild-type and *swf1*Δ cells have a similar number of cortical F-actin patches. By 2 min post-LatA addition, actin patches were no longer observed in LatA-treated *swf1*Δ cells, although actin patches were observed readily in LatA-treated wild-type cells at this time point (Figure 3B). Thus, it seems that Swf1p slows actin turnover in vivo and that the organizational defects of the actin cytoskeleton in cells lacking *SWF1* may be due to altered actin dynamics.

Swf1p Colocalizes with Cortical Actin Patches

The regulation of the actin cytoskeleton by *SWF1* suggested that Swf1p associates in vivo with one or more actin structures. We found that Swf1p colocalizes with cortical actin patches and actin cables (Figure 4). Our initial attempts to localize Swf1p with real-time imaging, by using a GFP fusion tag, proved unsuccessful. Only when wild-type cells were fixed and probed with a polyclonal antibody against GFP was GFP-Swf1p localization possible. We found GFP-Swf1p in cortical puncta of faint intensity (Figure 4A). During, but independent of our study, Valdez-Taubas and Pelham (2005) reported the localization of GFP-Swf1p at the endoplasmic reticulum. This difference in Swf1p localization is considered further in *Discussion*. To take a different route toward determining where Swf1p localizes, we raised a polyclonal antibody against the C-terminal region of Swf1p. This antibody displayed affinity for the immunogen (GST-Swf1-C) but not GST (Supplemental Figure 2). On immunoblots of whole cell lysates, this antibody recognized a polypeptide of ~40 kDa, which is the predicted molecular weight of Swf1p and consistent with the migration of myc-tagged Swf1p in SDS-PAGE gels (Ohno *et al*., 2006). This polypeptide of ~40 kDa was detectable in whole cell lysates of wild-type cells but not of mutant cells lacking *SWF1* (Figure 4B). Even with purification, the antibody we raised against Swf1p exhibited cross-reactivity with other polypeptides on immunoblots. Such cross-reactivity, however, was not apparent in cells prepared for indirect immunofluorescence microscopy. On probing wild-type haploid (data not shown) and diploid (data shown) cells with purified Swf1-C antibody, we found that Swf1p localizes primarily to small cortical puncta (Figure 4C, left). A faint filamentous fluorescent signal was also observed in some cells (arrowheads in Figure 4C). Neither localization pattern was observed in cells lacking Swf1p (Figure 4C, right). The Swf1p localization pattern was consistent among our laboratory strains as well as in a BY4742-derived diploid (KKY1120; data not shown). As with our localization of GFP-Swf1p, antibody against Swf1p did not detect an accumulation of Swf1p in the cell body suggestive of an accumulation at the endoplasmic reticulum.

After establishing the localization of Swf1p, we double labeled diploid wild-type cells for Swf1p and actin. We found that Swf1p colocalizes with most but not all cortical actin patches (Figure 4D). In control staining reactions that used both secondary antibodies and either of the primary antibodies (data not shown), localization of Swf1p or actin was dependent upon the presence of the cognate primary antibody. No cross-reactivity between mismatched secondary and primary antibodies was observed either. In double label experiments, some cells also exhibited a uniform faint signal for Swf1p along the length of actin cables (Figure 4D). The localization of Swf1p was actin dependent (Figure 4E). When wild-type cells were treated for 10 min with 400 μM LatA, a drug that depolymerizes F-actin structures, Swf1p was no longer observed on cytoplasmic filaments and only a faint Swf1p signal remained at a few cortical puncta (arrowheads in Figure 4E, bottom left). LatA treatment did not globally abolish the localization of proteins at sites of polarized growth. The septin Cdc11p, for example, remained at the incipient bud site and mother-bud neck in the LatA-treated cells (Figure 4E, right). Although these data do not show unequivocally a direct interaction of Swf1p with actin, they do indicate that Swf1p associates with F-actin structures, especially on the cell cortex at sites of endocytosis.

To determine whether Swf1p binds actin directly, we tested whether the C-terminal region (residues 235–336) of Swf1p, which is predicted to be cytoplasmic (Politis *et al*., 2005), bound F- or G-actin. Due to protein instability, we were unable to assay recombinant full-length Swf1p. In a supernatant depletion assay, we found that the Swf1p C-terminal domain when fused to GST (GST-Swf1-Cp) did not cosediment with F-actin in a concentration-dependent manner (Supplemental Figure 3A). In a pyrene–actin assembly assay, we found that GST-Swf1-Cp in molar excess to G-actin did not affect actin assembly (Supplemental Figure 3B). Both of these results indicate that the C-terminal domain of

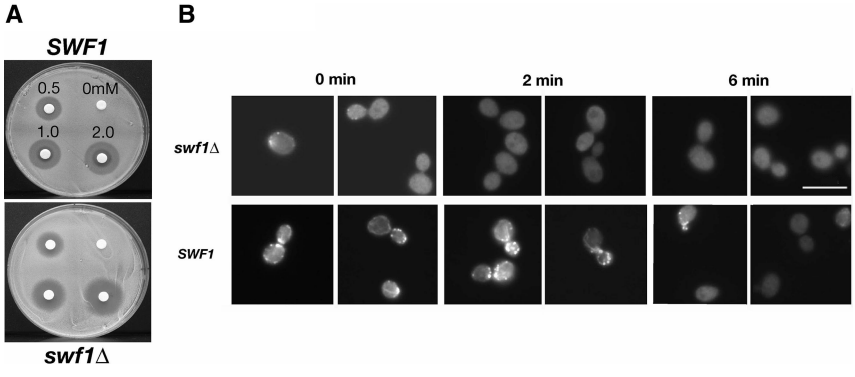

Figure 3. Actin turnover was more rapid in the absence of *SWF1*. (A) Halo assay that showed the sensitivity of a haploid wild type strain (KKY1064) and *swf1*Δ mutant strain (KKY1063), grown at 25°C on rich medium, LatA. Counterclockwise, filter disks were impregnated with 0, 0.5, 1, and 2 mM LatA. (B) Micrographs of an in vivo actin turnover assay that showed a higher rate of actin turnover in *swf1*Δ mutant strain (KKY1090) compared with a wild-type strain (DDY663). We added 0.4 mM LatA at time zero, at which time, and at 2 and 6 min postdrug addition, aliquots of each culture were collected and stained with rhodamine-phalloidin. Rhodamine-phalloidin staining of nontreated cells looked like that shown in Figure 8A. Bar, 5 μm.

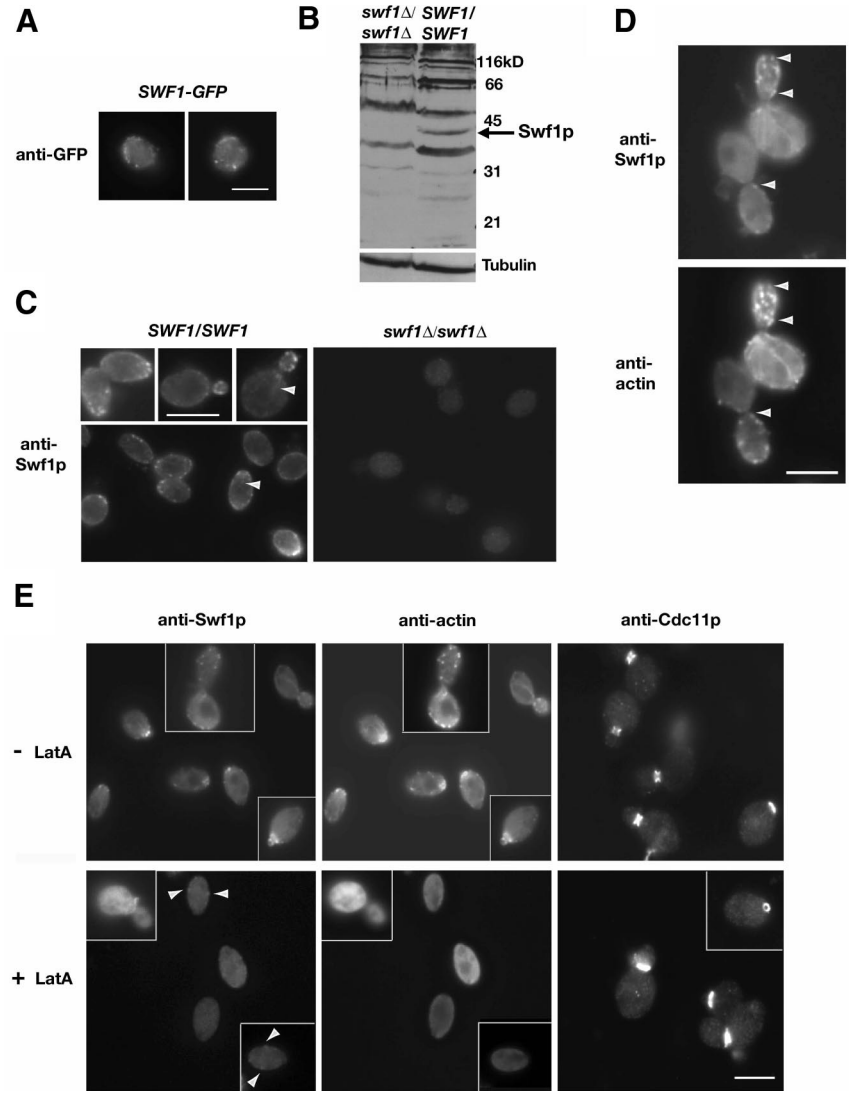

Figure 4. Swf1p colocalized with cortical actin patches. (A) Indirect immunofluorescence micrographs of log phase wild-type cells expressing *SWF1-GFP* (KKY1104) labeled with anti-GFP and goat anti-rabbit-FITC antibodies. (B) Immunoblot of whole cell extract of log phase mutant *swf1*Δ/*swf1*Δ (KKY1060; right) and wild-type *SWF1/SWF1* (DDY1102) diploid cells, grown at 25°C in rich medium, and probed with a polyclonal antibody against the C terminus of Swf1p. To demonstrate equivalent loading, the same blot was probed with an antibody against β-tubulin. (C) Indirect immunofluorescence micrographs of log phase wild-type *SWF1/SWF1* (DDY1102; left) and mutant *swf1*Δ/*swf1*Δ (KKY1060; right) diploid cells, grown at 25°C in rich medium, and labeled with the same anti-Swf1p antibody used in B and goat anti-rabbit-Alexa 568. Arrowheads mark filamentous structures detected by the Swf1p antibody. (D) Indirect immunofluorescence micrographs of log phase wild-type cells (DDY1102) double labeled with polyclonal antibodies against Swf1p and actin. Goat anti-rabbit FITC and donkey anti-guinea pig-rhodamine served as secondary antibodies. Arrowheads mark examples of Swf1p and actin colocalization. (E) Indirect immunofluorescence micrographs of log phase wild-type *SWF1/SWF1* (DDY1102; left) diploid cells cultured at 25°C in rich medium for 10 min with (bottom row) and without (top row) 400 μM LatA. The left and middle panels in each row show the same cells double labeled as in D. Arrowheads in bottom left panel mark examples of Swf1p localization. The panels on the right show cells from the same culture, with and without LatA, probed with anti-septin (Cdc11p) and goat anti-rabbit-Alexa 568 antibodies. Bars, 5 μm.

Swf1p, when bound to GST, is unable to bind either F- or G-actin, suggesting that Swf1p does not bind actin directly.

Cdc42p Mislocalizes in the Absence of Swf1p

Next, we examined whether the localization of Cdc42p depends upon Swf1p. Cdc42p sits atop a hierarchy of signal transduction events that lead to polarized cell growth (Park and Bi, 2007). Localization of Cdc42p at the incipient bud site in unbudded cells or at the apical bud cortex in small- and medium-budded cells is necessary for proper cell polarization (Ziman *et al*., 1991). Both the genetic interactions observed between *SWF1* and *CDC42* and the loss of cytoskeletal polarity in *swf1*Δ and *swf1*Δ/*swf1*Δ mutants suggested that Cdc42p depends upon Swf1p for proper localization. We found little difference in Cdc42p localization in unbudded and small-budded wild-type and *swf1*Δ cells (Figure 5). Among small-budded cells, 100 and 92% of wild-type and *swf1*Δ cells, respectively, showed proper Cdc42p localization on the bud cortex. However, a significant difference was observed with medium-budded cells (Figure 5B). We found that 97% of medium-budded wild-type cells had proper Cdc42p localization on the bud cortex, whereas only 13% of the medium-budded *swf1*Δ cells had properly localized Cdc42p (Figure 5B). In mutant cells, Cdc42p localized normally to the apical bud tip but also abnormally to large patches within the mother cell, proximal to the mother-bud neck (Figure 5A). Similar localization patterns were found in homozygous *swf1*Δ diploid cells as well (Figure 5A). These data indicate that the polarized localization of Cdc42p is dependent upon Swf1p during a specific phase (S/G2) of the cell cycle.

*swf1*Δ *Cells Are Defective in Secretion and Accumulate Vesicles*

Two observations led to a prediction that cells lacking *SWF1* are defective in polarized secretion. First, actin cables, along which secretory vesicles move, were fewer in cells lacking *SWF1*, compared with wild-type cells (Bonangelino *et al*., 2002; this study). Second, the SNARE Tlg1p, which is part of the exocytotic apparatus (Holthuis *et al*., 1998), is degraded in cells lacking *SWF1* (Valdez-Taubas and Pelham, 2005). We found two lines of evidence that show *swf1*Δ cells are defective in polarized secretion. First, thin section electron microscopic analysis revealed an accumulation of 80- to 100-nm vesicles in the buds of two independently derived *swf1*Δ strains, KKY1063 (Figure 6, bottom) and 1-7-11 (data not

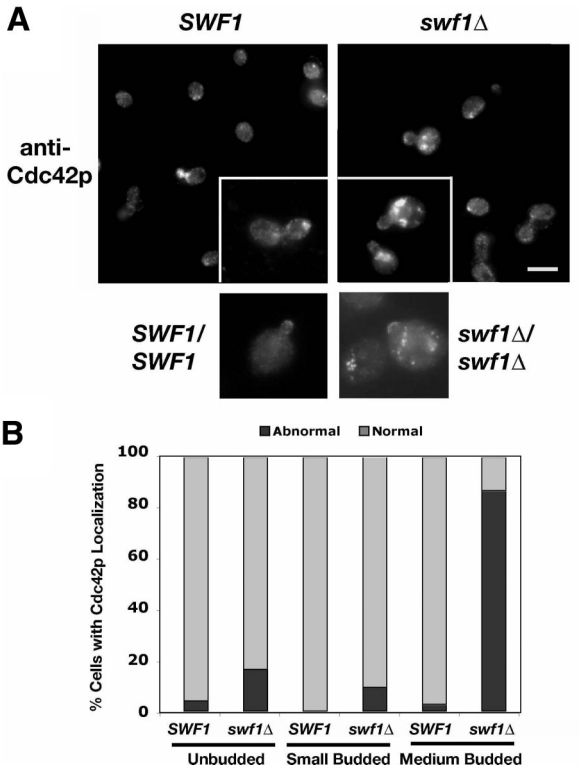

Figure 5. Cdc42p mislocalized in the absence of Swf1p. (A) Indirect immunofluorescence micrographs of log-phase haploid *SWF1* (KKY1064; top left and inset) and *swf1*Δ (KKY1063; top right and inset) cells as well as diploid *SWF1/SWF1* (DDY 1102; bottom left) and *swf1*Δ/*swf1*Δ (KKY1060; bottom right) cells, grown at 25°C in rich medium, labeled with anti-Cdc42p and goat anti-rabbit-Alexa 568 antibodies. Bar, 5 μm. (B) Comparison of the number of haploid *SWF1* and *swf1*Δ cells with a proper localization of Cdc42p at different cell cycle stages. Cdc42p localization was scored as properly localized or normal when it was found as a patch or crescent on the cortex of unbudded cells or at the apical bud tip of small- and medium-budded cells. Bright patches of Cdc42p staining at noncortical locations were scored as abnormal. All scored cells had single nucleus as visualized with DAPI. n >174 cells scored for each strain. The cells quantified were from the same experiment shown in A.

shown; BY4742 background). Accumulation of 80- to 100-nm vesicles is a signature phenotype of impaired exocytosis. For example, *sec6-4*^{ts} cells, which served as our positive control for detecting secretory vesicles in thin section, have a tight exocytotic block at 37°C (Novick *et al*., 1980; Harsay and Bretscher, 1995). After being shifted from 25°C to 37°C for 120 min, *sec6-4*^{ts} cells failed to bud and accumulated 80- to 100-nm vesicles (Figure 6, top right). In contrast to the *swf1*Δ strain, in which vesicles accumulated in the buds, few if any vesicles were observable in the buds of wild-type cells (Figure 6, top left). As with the wild-type strain, the mother cells of the *swf1*Δ strain did not contain an accumulation of vesicles. These results indicate that *SWF1* is not required for vesicle transport to the bud and strongly suggest that *SWF1* is necessary for efficient exocytosis from the bud.

Consistent with this observation and the prediction *swf1*Δ cells are defective in polarized secretion, we found an internal accumulation of β-1,3-glucanase (Bgl2p) in *swf1*Δ cells (Figure 7). Bgl2p is a cell wall remodeling enzyme that is secreted to the plasma membrane (Harsay and Bretscher, 1995). On assaying the internal Bgl2p pool in wild-type cells, cells lacking *SWF1*, and *sec6-4*^{ts} cells grown at 25°C or shifted from 25 to 37°C, we found no appreciable accumulation of Bgl2p in wild-type cells cultured at either temperature, and we found a significant accumulation of Bgl2p in *sec6-4*^{ts} control cells only after shift to restrictive temperature. In *swf1*Δ cells, Bgl2p accumulated to the level observed in *sec6-4*^{ts} grown at 37°C. This accumulation was not temperature dependent. The results of this Bgl2p assay and our electron microscopy data indicate that *swf1*Δ cells have a defect in polarized secretion, occurring late in the secretory pathway.

Actin Organization and Cdc42 Localization Are Independent of the Swf1p DHHC Motif

Valdez-Taubas and Pelham (2005) observed that deletion of the ubiquitin ligase Tul1p did not suppress all *swf1*Δ phenotypes such as the inability of *swf1*Δ cells to grow on lactate. This observation suggested that Swf1p has multiple distinct functions. Because of this observation, we asked whether the ability of Swf1p to promote the polarization of the actin cytoskeleton was dependent on the DHHC motif. Earlier studies demonstrated that substitution of cysteine in the DHHC motif with alanine abolished the palmitoyltransferase (PT) activity of DHHC-CRD family palmitoyltransferases (Lobo *et al*., 2002; Roth *et al*., 2002), or, in Swf1p, the DHHC motif was necessary for SNARE palmitoylation (Valdez-Taubas and Pelham, 2005). To address this question, we examined by fluorescence microscopy the organization of the actin cytoskeleton in cells solely expressing either wild-type Swf1p (DHHC) or Swf1p with a mutated DHHC motif (DHHA). Wild-type and mutant Swf1p were expressed from a low copy *CEN* plasmid in *swf1*Δ cells. We found that cells expressing Swf1-DHHAp had a wild-type morphology and that the actin cytoskeleton remained polarized, similar to cells expressing Swf1-DHHCp (Figure 8, A and B). Likewise little variation in actin polarization was observed among populations of unbudded cells. In the same experiment, we tried to compare actin polarization in cells expressing Swf1-DHHAp to that found in a *swf1*Δ strain containing only vector. We found, however, that liquid minimal medium did not support the growth of *swf1*Δ cells containing an empty vector. Therefore, cells expressing Swf1-DHHAp were compared with a *swf1*Δ strain and a *SWF1* strain grown in rich medium. The number of Swf1-DHHCp and Swf1-DHHAp transformants with a polarized actin cytoskeleton closely resembled that of *SWF1* cells, indicating that expression of *SWF1* from a plasmid did not affect its function. Together, these results showed that the DHHC motif of Swf1p is not necessary for promoting the polarized organization of the actin cytoskeleton.

The polarized organization of the actin cytoskeleton in cells solely expressing Swf1-DHHAp suggested that mutation of the DHHC motif does not affect actin dynamics. To test this idea, we compared the sensitivity of cells expressing either Swf1-DHHCp or Swf1-DHHAp to LatA in a halo assay. As shown in Figure 8C, we found no apparent increase in sensitivity to LatA between a strain expressing Swf1-DHHAp to a strain expressing Swf1-DHHCp. This result suggested that substitution of the cysteine in the DHHC motif does not affect actin dynamics.

Wild-type actin organization in cells expressing only Swf1-DHHAp implied that the DHHC motif is not necessary for the proper localization of Cdc42p at sites of polarized growth. To test whether Cdc42p, a key regulator of actin organization at polarized growth sites, localized properly in cells with a DHHA motif, we probed cells expressing either Swf1-DHHCp or Swf1-DHHAp with an antibody against Cdc42p. We found a wild-type pattern of Cdc42p localiza-

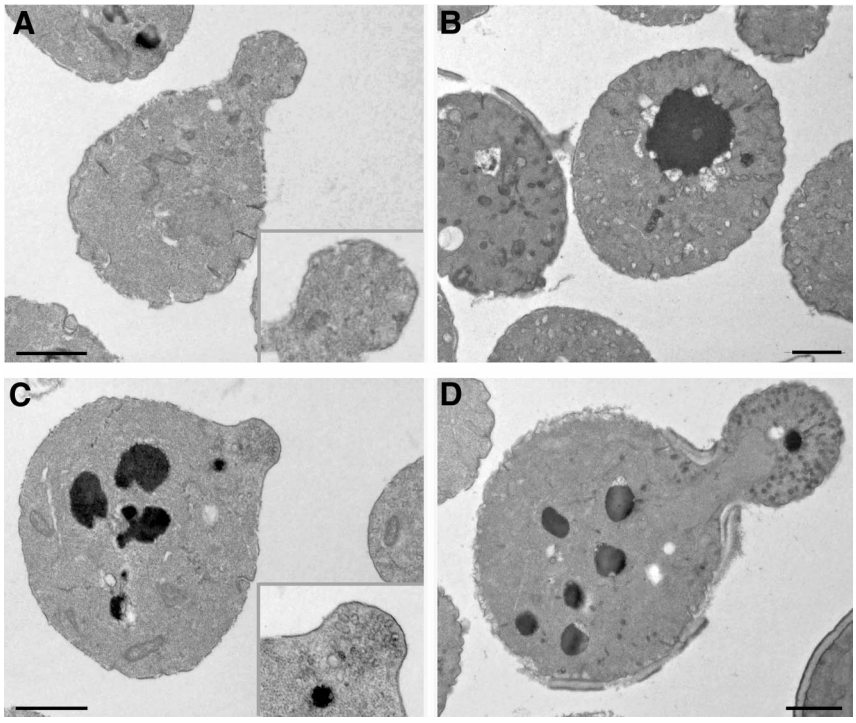

Figure 6. Vesicles (80–100 nm) accumulated in the buds of cells lacking *SWF1*. Electron micrographs show thin sections of wild-type *SWF1* (KKY1064) (A), *sec6-4*^{ts} (NY17) (B), and *swf1*Δ (KKY1063) (C and D) log phase cells cultured in rich medium. Strains shown in A, C, and D were cultured at 25°C; the strain shown in B was cultured at 37°C. Insets show an enlarged image of a bud. Bar, 5 μm.

tion in cells expressing Swf1-DHHAp (Figure 8D). Therefore, the Swf1p DHHC motif is not necessary for the proper localization of Cdc42p.

Loss of the Swf1p DHHC Motif Differentially Affects Secretion

Because abnormalities were not observed in the organization or dynamics of the actin cytoskeleton in cells expressing Swf1p with a mutated DHHC motif (DHHA), we asked whether the secretion of Bgl2p was blocked in these mutant cells. That is, we sought to determine whether the secretion defect in *swf1*Δ cells was due to a change in the actin cytoskeleton or due to a change in the palmitoylation state of SNAREs. To address this question, we first assayed Bgl2p secretion in cells expressing no Swf1p (*swf1*Δ), wild-type Swf1p (DHHC), or Swf1p with a mutated DHHC motif (DHHA). As a control for Bgl2p secretion, we included a *sec6-4*^{ts} strain in our analysis. This strain is temperature-conditional for secretion and accumulates Bgl2p internally after shift from 25 or 37°C (Harsay and Bretscher, 1995). We found that at both 25 or 37°C, the amount of Bgl2p that accumulated internally in *swf1-DHHA* cells, which display no actin defects, was very similar to the amount of Bgl2p that accumulated in wild-type cells (Figure 8E). Furthermore, the amount of Bgl2p that accumulated internally in cells expressing either wild-type (DHHC) or mutant (DHHA) Swf1p was much lower than the amount of Bgl2p in *swf1*Δ cells, which lack Swf1p entirely. These results indicate that Swf1p DHHC motif is not necessary for Bgl2p secretion and suggest that the defect in Bgl2p secretion in *swf1*Δ cells may result from a defect in actin organization.

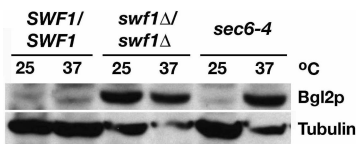

Figure 7. The secretory marker Bgl2p accumulated internally in the absence of *SWF1*. Immunoblot shows from left to right the internal level of secretory pathway marker Bgl2p, in log phase wild-type *SWF1/SWF1* (DDY1102) and *swf1*Δ/*swf1*Δ (KKY 1060), and *sec6-4*^{ts} (NY17) cell, cultured for 90 min at 25 or 37°C in rich medium. To demonstrate equivalent loading, the same blot was probed with an antibody against β-tubulin.

Wild-type Bgl2p secretion in cells with a mutated Swf1p DHHC motif contradicted the idea that the DHHC motif, and by inference Swf1p PT activity, is physiologically relevant to secretion. To determine whether the Swf1p DHHC motif is relevant to any type of secretion as predicted from the ability of Swf1p to palmitoylate specific SNAREs, we performed an additional secretion assay. With the same strains used for the Bgl2p assay described above, we assayed the secretion of invertase (Table 3). We found that deletion of *SWF1* impaired secretion at 25°C, in comparison with wild-type (Student's *t* test, $p = 0.06$). Transformation of *swf1*Δ cells with a plasmid containing wild-type *SWF1* rescued the mutant phenotype. Therefore, no significant difference in invertase secretion was observed whether Swf1p was expressed from a low copy plasmid (+ DHHC) in a *swf1*Δ strain or from a chromosomal copy of the gene (*SWF1*). In contrast, the *swf1*Δ phenotype with respect to invertase secretion was not rescued by plasmid-borne *swf1-DHHA*. The average ratio of secreted invertase to total invertase in cells expressing Swf1p without a DHHC motif (*swf1*Δ + DHHA) was significantly less (Student's *t* test, $p = 0.01$) than that measured for cells expressing wild-type Swf1p (*swf1*Δ + DHHC), 0.64 versus 0.77, respectively. None of the *swf1* mutants showed a secretory block as severe as that of *sec6-4* cells shifted from 25to 37°C, in which the average ratio of secreted to total invertase fell from 0.82 to 0.13. Together, these data demonstrate that cells expressing Swf1p without a DHHC motif are defective in secretion in the invertase-

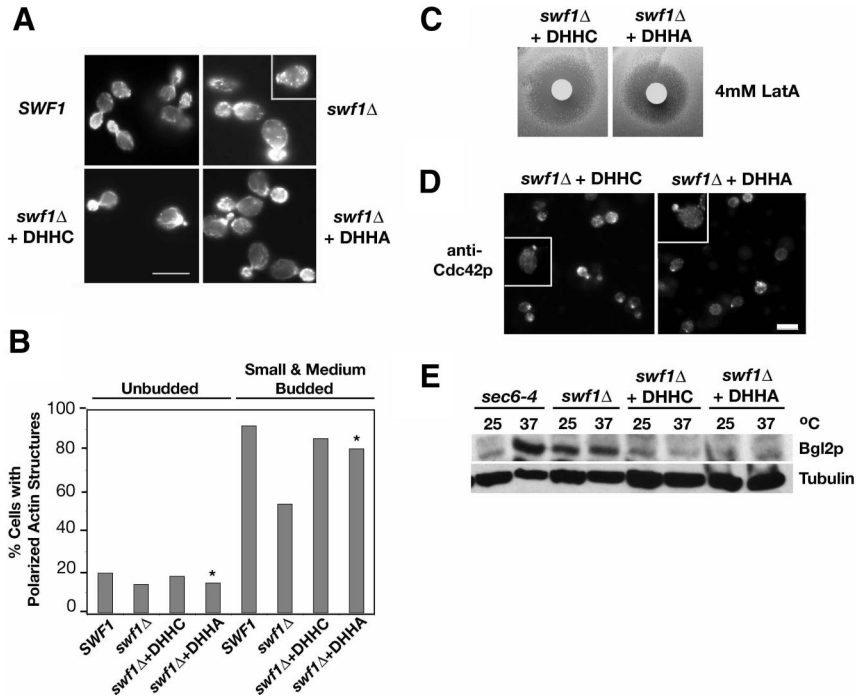

Figure 8. Actin organization, Cdc42p localization, and Bgl2p-marked secretion were independent of the Swf1p DHHC motif. (A) Micrographs of rhodamine-phalloidin-stained, log phase, haploid, wild-type *SWF1* cells (KKY1064), mutant *swf1*Δcells (KKY 1063), and *swf1*Δ cells with *CEN* plasmid that contained wild-type (+DHHC; KKY1086) or mutant *SWF1* (+DHHA; KKY1087). All strains were grown at 25°C. *SWF1* and *swf1*Δ stains were grown on rich medium and *swf1*Δ strains containing a plasmid were grown in SC-URA. Bar, 5 μm. (B) Comparison of the number of cells with polarized cortical actin cytoskeleton, at different cell cycle phases. The cortical actin cytoskeleton was scored as polarized when cortical actin patches were distributed to one pole of unbudded cells or were distributed to the bud in small- and medium-budded cells. All scored cells had a single nucleus as visualized with DAPI. n > 200 cells scored for each morphological class. The cells quantified were from the same experiment shown in A. Asterisks highlight the strain that lacked the DHHC motif. (C) Halo assay with the same strains used in A plated on SC-Ura and incubated at 25°C for 2 d. Filter disks were impregnated with 4 mM LatA. (D) Indirect immunofluorescence micrographs of log-phase *swf1*Δ cells expressing Swf1-DHHCp (KKY1086; left) or Swf1-DHHAp (KKY1087; right), grown at 25°C in SC-Ura, labeled with anti-Cdc42p and goat anti-rabbbit-Alexa 568 antibodies. Bar, 5 μm. (E) Immunoblot shows from left to right the internal level of secretory marker Bgl2p in log phase *sec6-4*^{ts} (NY17), *swf1*Δ (KKY1063), *swf1*Δ + DHHC (KKY1086), and *swf1*Δ + DHHA (KKY 1087) cells, cultured for 90 min, at 25 or 37°C in rich and SC-Ura medium. To demonstrate equivalent loading, the same blot was probed with an antibody against β-tubulin.

marked secretory pathway, but not the Bgl2p-marked pathway.

The Swf1p DHHC Motif Is Functionally Relevant to a Growth-related Cdc42p Function

The demonstrated independence of actin organization, Bgl2p-marked secretion, and Cdc42p localization from the Swf1p DHHC motif predicted that the DHHC motif is not functionally relevant to the function of Cdc42p in polarized growth. That is, mutation of the DHHC motif would not enhance *cdc42* growth defects. To test this prediction, we compared at a range of temperatures the growth of *cdc42*^{ts} *swf1*Δ double mutants that contained an empty plasmid vector with those that contained plasmid-borne *swf1*-DHHA (Figure 9). Double mutant strains that contained plasmid-borne wild-type *SWF1* defined the temperature range of individual *cdc42*^{ts} alleles under the growth conditions used.

Contrary to our prediction, we found that the DHHC motif of Swf1p is functionally relevant to Cdc42p function during polarized cell growth. We observed that the Swf1p DHHC motif is necessary for the rescue of two of three different *cdc42*^{ts} *swf1*Δ synthetic genetic interactions (Figure 9). A *cdc42-118 swf1*Δ strain that contained plasmid-borne *swf1-DHHA* exhibited the same permissive temperature range for growth as one with an empty vector. A similar result was observed with *cdc42-129*. Because *cdc42-129* and *swf1*Δ are lethal in combination (Figure 1B), we asked whether we could recover viable double mutants with plasmid-borne *swf1-DHHA*, upon sporulation of a double heterozygote transformed with a plasmid containing *swf1-DHHA*. We found that we were unable to recover, after meiosis at 25°C, *cdc42-129 swf1*Δ progeny with either empty vector or plasmid-borne *swf1-DHHA*. In contrast, *cdc42-129 swf1*Δ progeny with plasmid-borne *SWF1* were easily recoverable. These data indicate that the DHHC motif is functionally relevant to at least one growth-related function of Cdc42p.

In the converse case, where *swf1*Δ suppresses rather than exacerbates a *cdc42* temperature-sensitive growth defect, we observed that a *cdc42-101 swf1*Δ strain that contained plasmid-borne *swf1-DHHA* exhibited the same permissive temperature range for growth as a strain with plasmid-borne wild-type *SWF1*. Although equivalent growth of a *cdc42 swf1*Δ mutant containing either *swf1-DHHA* or wild-type *SWF1* would normally indicate that a functional DHHC motif is not required for the rescue of the double mutant growth phenotype, it is important to note that the double

Table 3. Invertase secretion in wild-type and *swf1* cells

Genotype	Mean secreted/total invertase	n samples	n independent assays
At 25°C			
SWF1	0.78 ± 0.03	10	6
*swf1*Δ	0.69 ± 0.03	7	5
sec6-4	0.82 ± 0.04	8	5
*swf1*Δ + DHHC	0.77 ± 0.04	9	5
*swf1*Δ + DHHA	0.64 ± 0.02	10	5
At 37°C			
sec6-4	0.13 ± 0.02	14	7

Invertase activity (in A_{540} units) was measured as described in *Materials and Methods*. A SE is given for each mean. The strains used for this assay were *SWF1* (KKY1064), *swf1*Δ (KKY1063), *sec6-4* (NY17), *swf1*Δ + DHHC (KKY1086), and *swf1*Δ + DHHA (KKY1087).

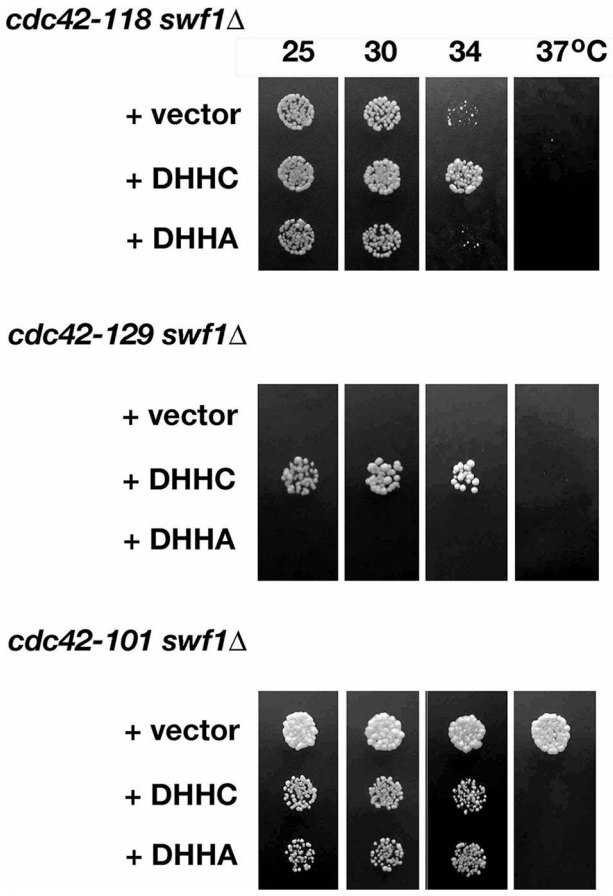

Figure 9. Synthetic genetic interactions between certain *cdc42*^{ts} alleles and *swf1*Δ required the Swf1p DHHC motif. Equivalent dilutions of *swf1*Δ *cdc42-118*, *swf1*Δ *cdc42-129*, and *swf1*Δ *cdc42-101* strains were plated and grown at 25, 30, and 37°C for 3 d on SC-Ura. These strains contained a *CEN* plasmid vector that was either empty or filled with wild-type *SWF1* (DHHC) or *swf1* in which the DHHC motif was mutated (DHHA). The strains shown (from top to bottom) are KKY1137, 1138, 1139, 1140, 1134, 1135, and 1136. Note that no *swf1*Δ *cdc42-129* cells containing vector or plasmid-borne *swf1-DHHA* were plated because neither the vector nor *swf1-DHHA* suppressed the synthetic lethal interaction between *swf1*Δ and *cdc42-129*.

mutant in this case has an expanded growth range. This result suggests that a part of Swf1p, other than the DHHC motif, counterbalances a Cdc42p function related to growth.

DISCUSSION

Temperature-conditional *cdc42* mutants in *S. cerevisiae* have proven incredibly valuable for the identification of conserved genes and gene families that regulate *CDC42*-dependent polarized cell growth (Kozminski *et al*., 2003; Kozminski *et al*., 2006). Herein, we demonstrated that one such gene, *SWF1*, is necessary for proper cell polarization. Although the exact biochemical mechanism by which Swf1p regulates cell polarization remains unknown, we found that several cellular processes depend upon Swf1p. Swf1p is necessary for the polarized localization of the Rho-family GTPase Cdc42p, the polarization of the actin cytoskeleton, and for trafficking along a specific secretory pathway. To our surprise, none of these processes depend upon the DHHC motif in Swf1p and, by extension, the PT activity that Swf1p is very likely to possess.

GTPase localization, cytoskeletal polarization, and vesicle trafficking are intimately related processes that are necessary for proper polarized cell growth in yeast (Park and Bi, 2007). In unbudded G1 cells, the localization and activation of Cdc42p at the incipient bud site is essential for the polarized organization of the actin cytoskeleton (Sloat *et al*., 1981; Adams *et al*., 1990; Ziman *et al*., 1991, 1993; Gulli *et al*., 2000; Richman and Johnson, 2000) and the establishment of polarized secretion (Adamo *et al*., 2001; Zhang *et al*., 2001; Roumanie *et al*., 2005; Zajac *et al*., 2005). In small- and medium-budded cells, in S and G2/M, respectively, the maintenance of Cdc42p localization at the bud tip depends upon a properly polarized actin cytoskeleton and polarized secretion. Mutations or drugs that disrupt either process disrupt the polarized distribution of Cdc42p (Wedlich-Soldner *et al*., 2003; Irazoqui *et al*., 2005; Zajac *et al*., 2005). With few unbudded and small-budded *swf1*Δ and *swf1*Δ/*swf1*Δ cells displaying a loss of cytoskeletal organization or Cdc42p polarization, relative to medium-budded cells, we conclude that Swf1p does not affect the process of establishing an axis of polarized growth early in the cell cycle. Rather our data suggest that Swf1p functions, with respect to polarized cell growth, after bud emergence as part of the cellular mechanism that maintains a polarized distribution of Cdc42p during bud growth.

Thus far, our data are unable to reveal unequivocally in which process Swf1p acts primarily to promote polarized growth. For example, a loss of polarized secretion in *swf1*Δ mutants may result from an aberrant organization of the actin cytoskeleton, as is known to occur in *tpm1-2 tpm2* mutants (Pruyne *et al*., 1998). It is also possible that Swf1p functions in more than one process required for polarized cell growth, as suggested by the inability of *cdc42-DHHA* to rescue all *cdc42*^{ts} *swf1*Δ synthetic growth phenotypes. The identification of *SWF1* in multiple independent screens (Bartels *et al*., 1999; Bonangelino *et al*., 2002; Enyenihi and Saunders, 2003) shows that Swf1p can function in multiple processes (e.g., trafficking to the vacuole, spore wall formation). Taking these data and our own into consideration, the actin cytoskeleton stands out as a common denominator. Therefore, what may seem to be independent processes during polarized cell growth may be due to a single Swf1p activity affecting the actin cytoskeleton. In addition to our data that show Swf1p regulates the actin cytoskeleton, it should not be forgotten that *SWF1* was first reported as a gene that is synthetic lethal with a hypomorphic, although undesignated, allele of *PFY1* (Bartels *et al*., 1999). *PFY1* encodes profilin, a protein that regulates actin dynamics (Jockusch *et al*., 2007). We infer from the literature that the allele used in this screen was *pfy1-111* (Haarer *et al*., 1996). We have independently confirmed (our unpublished observations) this genetic interaction by using *pfy1-4*, an allele that encodes a mutant profilin defective in actin monomer binding (Wolven *et al*., 2000), whereas finding, within additional although small data sets, no synthetic lethality between *swf1*Δ and *PFY1* alleles specifically defective in functions other than actin monomer binding (e.g., binding to formin homology domain-containing proteins). Because synthetic genetic interactions often reveal a common function between proteins, we must consider whether Swf1p like Pfy1p binds actin monomers. Such biochemical activity is unlikely because Swf1p does not contain any known actin binding motifs. The region of Swf1p most likely to bind actin is the long C-terminal tail, which based on a membrane-spanning topology model of the DHHC-CRD protein Akr1p (Politis *et al*.,

2005) is predicted to be cytoplasmic. We did not find that this C-terminal region binds actin directly. Therefore, it is more probable that the ability of Swf1p to regulate the actin cytoskeleton is by way of protein intermediates. Analogy may be drawn from membrane-anchored cytoskeletons in metazoans, in which Band 4.1 protein and Ezrin/radixin/moesin proteins link ion channels and CD44, respectively, to cortical actin filaments (Denker and Barber, 2002) or in yeast, where during receptor mediated-endocytosis receptors are linked to the actin cytoskeleton by way of Sla1p or the epsin-related proteins Ent1/2p (Engqvist-Goldstein and Drubin, 2003).

Because profilin is a potent regulator of actin dynamics, it is tempting to speculate that the actin organization defects in *swf1*Δ cells is due to a perturbation of actin dynamics as has been observed in cells expressing mutant profilin (Wolven *et al*., 2000). Consistent with this idea, we noted, as in a previous study (Bonangelino *et al*., 2002), the paucity of actin cables in *swf1*Δ cells. We also observed a more rapid turnover of F-actin structures in *swf1*Δ cells in vivo in the presence of LatA. However, caution needs to be applied to the interpretation that Swf1p regulates actin dynamics. It is possible that the secretory defect observed in *swf1*Δ cells has altered the permeability of the cell wall to LatA, relative to wild-type cells. We have, in fact, observed (our unpublished observation) a slight sensitivity of *swf1*Δ cells to Calcofluor White, indicative of a defect in cell wall formation (Roncero *et al*., 1988). Unknown is whether this cell wall defect increases cell permeability to LatA to a physiologically significant level. Conversely, it is possible that a defect in the actin cytoskeleton leads to defective wall formation and in turn increased sensitivity to LatA (Gabriel and Kopecka, 1995). What is certain is that the organization, if not the dynamics, of the actin cytoskeleton depends upon Swf1p.

The localization of Swf1p to actin cables and patches is consistent with a role in the organization of the actin cytoskeleton. Why a predicted transmembrane protein is found on actin cables is not known. Cable-associated Swf1p may be derived from a pool of Swf1p associated with transport vesicles that move along actin cables or from a proteolytically processed domain of Swf1p (i.e., the C-terminal tail). Localization, however, is not proof of function at a particular locale. Localization at sites of endocytosis, for example, may solely reflect that Swf1p is concentrated at sites of endocytosis and is above the threshold of detection at these sites. It may be that Swf1p functions elsewhere. For example, Swf1p may function in endosomes or the late Golgi, where its substrate Tlg1p is known to reside (Lewis *et al*., 2000; Prescianotto-Baschong and Riezman, 2002). The appearance of Swf1p on the plasma membrane and subsequent endocytosis may be due to trafficking between endosomal compartments and the plasma membrane. In contrast, Valdez-Taubas and Pelham (2005) reported a different localization for Swf1p, showing that a GFP-Swf1p fusion protein localizes to the endoplasmic reticulum (ER). We did not find a similar pattern of localization with our indirect immunofluorescence technique, even using the same strain background as Valdez-Taubas and Pelham (2005). We speculate that the observed differences in Swf1p localization may be reflective of protein expression levels. Valdez-Taubas and Pelham (2005) drove expression of their tagged Swf1p with the strong constitutive *TPI1* promoter, whereas expression of Swf1p and Swf1-GFP in our study relied upon the endogenous *SWF1* promoter.

Our experiments directly showed that Swf1p has a role in secretion. During the course of our study, two independent investigations implicated Swf1p in secretion. In the first investigation, almost 40% (n = 26) of the genes identified in a synthetic lethal screen with *swf1*Δ by Tong *et al*. (2004) encode proteins known to function in the Golgi or in post-Golgi trafficking pathways. In the second investigation, Valdez-Taubas and Pelham (2005) showed that the palmitoylation of specific SNARE proteins depends upon Swf1p. In our study, we show that Swf1p is necessary for secretion along two different secretory pathways, one marked by invertase and the other marked by Bgl2p. In the absence of Swf1p, vesicles with a diameter signature of secretory vesicles accumulate in the bud, indicative of a block in late secretory pathway(s). These results are consistent with the study of Valdez-Taubas and Pelham (2005), which showed that Swf1p regulates the stability of the SNARE Tlg1p. When we expressed Swf1p with a mutated DHHC motif, invertase secretion was inhibited. Secretion along the Bgl2p-marked pathway, which is a secretory pathway that supports polarized cell growth, was not inhibited by mutation of the DHHC motif. These results provided several insights into Swf1p and polarized cell growth. First, secretion along the Bgl2p transport pathway, but not the invertase pathway, is independent of the Swf1p DHHC motif, indicating Swf1p has two distinct functions in regard to secretion. The data further suggest that the SNARE Tlg1p functions specifically within the invertase-marked secretory pathway. If, however, Tlg1p also functions within the Bgl2p-marked secretory pathway, it does so in a manner independent of the Swf1p DHHC motif. Second, in *swf1* mutant cells, defects in the actin cytoskeleton correlate more closely with defects in Bgl2p-marked secretion than invertase secretion. As stated above, it has not yet been possible to distinguish in *swf1* mutants whether a defect in Bgl2p secretion leads to an aberrant actin cytoskeleton or vice versa. What is clear is that Bgl2p-marked secretion and regulation of the actin cytoskeleton functions independently of the DHHC motif and, by inference, PT activity.

Palmitoylation is a posttranslational modification that contributes to the stability and trafficking of specific proteins (Linder and Deschenes, 2007). When in the course of our study it became known that Swf1p contributes to PT activity (Valdez-Taubas and Pelham, 2005), it became apparent to consider whether palmitoylation affected the intracellular distribution of Cdc42p. It is known the distribution of Ras between ER and plasma membrane depends upon the compartment specific palmitoylation of the G protein (Rocks *et al*., 2005). Furthermore, sequence analysis predicts the palmitoylation of two *S. cerevisiae* proteins necessary for proper polarized cell growth, Rho1p and Rho3p (Roth *et al*., 2006). These GTPases are in the same family as Cdc42p. Unlike Rho1 and Rho3, Cdc42p does not have an identifiable palmitoylation site. More importantly, we found that the distribution of Cdc42p in cells with a mutated DHHC motif was indistinguishable from that of cells expressing wild-type Swf1p. Therefore, it does not seem that the polarized localization of Cdc42p at the plasma membrane is dependent on palmitoylation.

Swf1p is among the family of seven transmembrane proteins in *S. cerevisia*e that contain a DHHC-CRD domain (Linder and Deschenes, 2007). It remains to be seen whether other DHHC-CRD proteins have a role in polarized cell growth, especially the regulation of the actin cytoskeleton. It is intriguing that no other genes that encode DHHC-CRD proteins were found in the synthetic genetic array screen that identified *SWF1* as *CDC42*-interacting, suggesting that the promotion of polarized cell growth may be a specific function of *SWF1*. In this regard, we have not tested directly the other DHHC-family members. Identifying the complete

range of Swf1p functions and that of other DHHC-CRD family members, although outside the scope of the current study, remains an important goal, considering the conservation of the DHHC-CRD protein family among plants, animals, and fungi (Putilina *et al*., 1999; Linder and Deschenes, 2003; Mitchell *et al*., 2006).

ACKNOWLEDGMENTS

We especially thank Edina Harsay (University of Kansas) for advice on secretion assays; Dorothy Schafer for help with actin binding assays; Anthony Bretscher (Cornell University), Anthony Frankfurter, Pekka Lappalainen (University of Helsinki), Mark Longtine (Washington University in St. Louis), David Pruyne (Cornell University), and Randy Schekman (University of California, Berkeley) for antibodies; David Drubin and P. Lappalainen for strains; and Jan Rednick (University of Virginia Central EM Facility) for assistance with electron microscopy. We also thank P. Lappalainen for a critical reading of the manuscript. National Science Foundation grant 0723342 and the University of Virginia provided support for this study.

REFERENCES

Adamo, J. E., Moskow, J. J., Gladfelter, A. S., Viterbo, D., Lew, D. J., and Brennwald, P. J. (2001). Yeast Cdc42 functions at a late step in exocytosis, specifically during polarized growth of the emerging bud. J. Cell Biol. *155*, 581–592.

Adams, A. E., and Pringle, J. R. (1991). Staining of actin with fluorochrome-conjugated phalloidin. Methods Enzymol. *194*, 729–731.

Adams, A. E. M., Johnson, D. I., Longnecker, R. M., Sloat, B. F., and Pringle, J. R. (1990). CDC42 and *CDC43*, two additional genes involved in budding and the establishment of cell polarity in the yeast *Saccharomyces cerevisiae*. J. Cell Biol. *111*, 131–142.

Alberts, P., Rudge, R., Irinopoulou, T., Danglot, L., Gauthier-Rouviere, C., and Galli, T. (2006). Cdc42 and actin control polarized expression of TI-VAMP vesicles to neuronal growth cones and their fusion with the plasma membrane. Mol. Biol. Cell *17*, 1194–1203.

Ayscough, K. R., Stryker, J., Pokala, N., Sanders, M., Crews, P., and Drubin, D. G. (1997). High rates of actin filament turnover in budding yeast and roles for actin in establishment and maintenance of cell polarity revealed using the actin inhibitor latrunculin-A. J. Cell Biol. *137*, 399–416.

Bankaitis, V. A., Malehorn, D. E., Emr, S. D., and Greene, R. (1989). The *Saccharomyces cerevisiae* SEC14 gene encodes a cytosolic factor that is required for transport of secretory proteins from the yeast Golgi complex. J. Cell Biol. *108*, 1271–1281.

Bartels, D. J., Mitchell, D. A., Dong, X., Deschenes, R. J. (1999). Erf2, a novel gene product that affects the localization and palmitoylation of Ras2 in *Saccharomyces cerevisiae*. Mol. Cell Biol. *19*, 6775–6787.

Belmont, L. D., and Drubin, D. G. (1998). The yeast V159N actin mutant reveals roles for actin dynamics *in vivo*. J. Cell Biol. *142*, 1289–1299.

Belmont, L. D., Patterson, G. M., and Drubin, D. G. (1999). New actin mutants allow further characterization of the nucleotide binding cleft and drug binding sites. J. Cell Sci. *112*, 1325–1336.

Bonangelino, C. J., Chavez, E. M., and Bonifacino, J. S. (2002). Genomic screen for vacuolar protein sorting genes in *Saccharomyces cerevisiae*. Mol. Biol. Cell *13*, 2486–2501.

Brachmann, C. B., Davies, A., Cost, G. J., Caputo, E., Li, J., and Boeke, J. D. (1998). Designer deletion strains derived from *Saccharomyces cerevisiae* 288C: a useful set of strains and plasmids for PCR-mediated gene disruption and other applications. Yeast *14*, 115–132.

Denker, S. P., and Barber, D. L. (2002). Ion transport proteins anchor and regulate the cytoskeleton. Curr. Opin. Cell Biol. *14*, 214–220.

Ducker, C. E., Stettler, E. M., French, K. J., Upson, J. J., and Smith, C. D. (2004). Huntingtin interacting protein 14 is an oncogenic human protein: palmitoyl acyltransferase. Oncogene *23*, 9230–9237.

Engqvist-Goldstein, A. E., and Drubin, D. G. (2003). Actin assembly and endocytosis: from yeast to mammals. Annu. Rev. Cell Dev. Biol. *19*, 287–332.

Enyenihi, A. H., and Saunders, W. S. (2003). Large-scale functional genomic analysis of sporulation and meiosis in *Saccharomyces cerevisiae*. Genetics *163*, 47–54.

Etienne-Manneville, S. (2004). Cdc42—the centre of polarity. J. Cell Sci. *117*, 1291–1300.

Fukata, M., Fukata, Y., Adesnik, H., Nicoll, R. A., and Bredt, D. S. (2004). Identification of PSD-95 palmitoylating enzymes. Neuron *44*, 987–996.

Gabriel, M., and Kopecka, M. (1995). Disruption of the actin cytoskeleton in budding yeast results in formation of an aberrant cell wall. Microbiology *141*, 891–899.

Garvalov, B. K., Flynn, K. C., Neukirchen, D., Meyn, L., Teusch, N., Wu, X., Brakebusch, C., Bamburg, J. R., and Bradke, F. (2007). Cdc42 regulates cofilin during the establishment of neuronal polarity. J. Neurosci. *27*, 13117–13129.

Gietz, R. D., and Sugino, A. (1988). New yeast-*Escherichia coli* shuttle vectors constructed with in vitro mutagenized yeast genes lacking six-base pair restriction sites. Gene *74*, 527–534.

Goldstein, A., and Lampen, J. O. (1975). Beta-D-fructofuranoside fructohydrolase from yeast. Methods Enzymol. *42*, 504–511.

Gulli, M. P., Jaquenoud, M., Shimada, Y., Niederhauser, G., Wiget, P., Peter, M. (2000). Phosphorylation of the Cdc42 exchange factor Cdc24 by the PAK-like kinase Cla4 may regulate polarized growth in yeast. Mol. Cell *6*, 1155–1167.

Haarer, B. K., Corbett, A., Kweon, Y., Petzold, A. S., Silver, P., and Brown, S. S. (1996). SEC3 mutations are synthetically lethal with profilin mutations and cause defects in diploid-specific bud-site selection. Genetics *144*, 495–510.

Harsay, E., and Bretscher, A. (1995). Parallel secretory pathways to the cell surface in yeast. J. Cell Biol. *131*, 297–310.

Harsay, E., and Schekman, R. (2007). Avl9p, a member of a novel protein superfamily, functions in the late secretory pathway. Mol. Biol. Cell *18*, 1203–1219.

Hill, K. L., Catlett, N. L., and Weisman, L. S. (1996). Actin and myosin function in directed vacuole movement during cell division in *Saccharomyces cerevisiae*. J. Cell Biol. *135*, 1535–1549.

Holthuis, J. C., Nichols, B. J., Dhruvakumar, S., and Pelham, H. R. (1998). Two syntaxin homologues in the TGN/endosomal system of yeast. EMBO J. *17*, 113–126.

Irazoqui, J. E., Howell, A. S., Theesfeld, C. L., and Lew, D. J. (2005). Opposing roles for actin in Cdc42p polarization. Mol. Biol. Cell *16*, 1296–1304.

Isgandarova, S., Jones, L., Forsberg, D., Loncar, A., Dawson, J., Tedrick, K., and Eitzen, G. (2007). Stimulation of actin polymerization by vacuoles via Cdc42p-dependent signaling. J. Biol. Chem. *282*, 30466–30475.

Jockusch, B. M., Murk, K., and Rothkegel, M. (2007). The profile of profilins. Rev. Physiol. Biochem. Pharmacol. *159*, 131–149.

Kozminski, K. G., Alfaro, G., Dighe, S., and Beh, C. T. (2006). Homologues of oxysterol-binding proteins affect Cdc42p- and Rho1p-mediated cell polarization in *S. cerevisiae*. Traffic *7*, 1224–1242.

Kozminski, K. G., Beven, L., Angerman, E., Tong, A. H., Boone, C., and Park, H. O. (2003). Interaction between a Ras and a Rho GTPase couples selection of a growth site to the development of cell polarity in yeast. Mol. Biol. Cell *14*, 4958–4970.

Kozminski, K. G., Chen, A. J., Rodal, A. A., and Drubin, D. G. (2000). Functions and functional domains of the GTPase Cdc42p. Mol. Biol. Cell *11*, 339–354.

Kroschewski, R., Hall, A., and Mellman, I. (1999). Cdc42 controls secretory and endocytic transport to the basolateral plasma membrane of MDCK cells. Nat. Cell Biol. *1*, 8–13.

Lappalainen, P. and Drubin, D. G. (1997). Cofilin promotes rapid actin filament turnover *in vivo*. Nature *388*, 78–82.

Lewis, M. J., Nichols, B. J., Prescianotto-Baschong, C., Riezman, H., and Pelham, H. R. (2000). Specific retrieval of the exocytic SNARE Snc1p from early yeast endosomes. Mol. Biol. Cell *11*, 23–38.

Linder, M. E., and Deschenes, R. J. (2003). New insights into the mechanisms of protein palmitoylation. Biochemistry *42*, 4311–4320.

Linder, M. E., and Deschenes, R. J. (2007). Palmitoylation: policing protein stability and traffic. Nat. Rev. Mol. Cell Biol. *8*, 74–84.

Lobo, S., Greentree, W. K., Linder, M. E., and Deschenes, R. J. (2002). Identification of a Ras palmitoyltransferase in *Saccharomyces cerevisiae*. J. Biol. Chem. *277*, 41268–41273.

Longtine, M. S., McKenzie, A., 3rd, Demarini, D. J., Shah, N. G., Wach, A., Brachat, A., Philippsen, P., and Pringle, J. R. (1998). Additional modules for versatile and economical PCR-based gene deletion and modification in *Saccharomyces cerevisiae*. Yeast *14*, 953–961.

Mitchell, D. A., Vasudevan, A., Linder, M. E., and Deschenes, R. J. (2006). Protein palmitoylation by a family of DHHC protein S-acyltransferases. J. Lipid Res. *47*, 1118–1127.

Mullins, R. D., Stafford, W. F., and Pollard, T. D. (1997). Structure, subunit topology, and actin-binding activity of the Arp2/3 complex from *Acanthamoeba*. J. Cell Biol. *136*, 331–343.

Nelson, W. J. (2003). Adaptation of core mechanisms to generate cell polarity. Nature *422*, 766–774.

Novick, P., Field, C., and Schekman, R. (1980). Identification of 23 complementation groups required for post-translational events in the yeast secretory pathway. Cell *21*, 205–215.

Ohno, Y., Kihara, A., Sano, T., and Igarashi, Y. (2006). Intracellular localization and tissue-specific distribution of human and yeast DHHC cysteine-rich domain-containing proteins. Biochim. Biophys. Acta *1761*, 474–483.

Palmgren, S., Ojala, P. J., Wear, M. A., Cooper, J. A., and Lappalainen, P. (2001). Interactions with PIP_2, ADP-actin monomers, and capping protein regulate the activity and localization of yeast twinfilin. J. Cell Biol. *155*, 251–260.

Park, H. O., and Bi, E. (2007). Central roles of small GTPases in the development of cell polarity in yeast and beyond. Microbiol. Mol. Biol. Rev. *71*, 48–96.

Peränen, J., Rikkonen, M., Hyvonen, M., and Kaariainen, L. (1996). T7 vectors with a modified T7*lac* promoter for expression of proteins in *Escherichia coli*. Anal. Biochem. *236*, 371–373.

Politis, E. G., Roth, A. F., and Davis, N. G. (2005). Transmembrane topology of the protein palmitoyltransferase Akr1. J. Biol. Chem. *280*, 10156–10163.

Prescianotto-Baschong, C., and Riezman, H. (2002). Ordering of compartments in the yeast endocytic pathway. Traffic *3*, 37–49.

Pringle, J. R. (1991). Staining of bud scars and other cell wall chitin with calcofluor. Methods Enzymol. *194*, 732–735.

Pringle, J., Preston, R., Adams, A., Stearns, T., Drubin, D., Haarer, B., and Jones, E. (1989). Fluorescence microscopy methods for yeast. Methods Cell Biol. *31*, 357–435.

Pruyne, D. W., Schott, D. H., and Bretscher, A. (1998). Tropomyosin-containing actin cables direct the Myo2p-dependent polarized delivery of secretory vesicles in budding yeast. J. Cell Biol. *143*, 1931–1945.

Putilina, T., Wong, P., and Gentleman, S. (1999). The DHHC domain: a new highly conserved cysteine-rich motif. Mol. Cell Biochem. *195*, 219–226.

Reneke, J. E., Blumer, K. J., Courchesne, W. E., and Thorner, J. (1988). The carboxy-terminal segment of the yeast α-factor receptor is a regulatory domain. Cell *55*, 221–234.

Richman, T. J., and Johnson, D. I. (2000). Saccharomyces cerevisiae Cdc42p GTPase is involved in preventing the recurrence of bud emergence during the cell cycle. Mol. Cell Biol. *20*, 8548–8559.

Rocks, O., Peyker, A., Kahms, M., Verveer, P. J., Koerner, C., Lumbierres, M., Kuhlmann, J., Waldmann, H., Wittinghofer, A., and Bastiaens, P. I. (2005). An acylation cycle regulates localization and activity of palmitoylated Ras isoforms. Science *307*, 1746–1752.

Roncero, C., Valdivieso, M. H., Ribas, J. C., and Duran, A. (1988). Isolation and characterization of *Saccharomyces cerevisiae* mutants resistant to Calcofluor white. J. Bacteriol. *170*, 1950–1954.

Roth, A. F., Feng, Y., Chen, L., and Davis, N. G. (2002). The yeast DHHC cysteine-rich domain protein Akr1p is a palmitoyl transferase. J. Cell Biol. *159*, 23–28.

Roth, A. F., Wan, J., Bailey, A. O., Sun, B., Kuchar, J. A., Green, W. N., Phinney, B. S., Yates, J. R., 3rd, and Davis, N. G. (2006). Global analysis of protein palmitoylation in yeast. Cell *125*, 1003–1013.

Roumanie, O., Wu, H., Molk, J. N., Rossi, G., Bloom, K., and Brennwald, P. (2005). Rho GTPase regulation of exocytosis in yeast is independent of GTP hydrolysis and polarization of the exocyst complex. J. Cell Biol. *170*, 583–594.

Salminen, A., and Novick, P. J. (1987). A ras-like protein is required for a post-Golgi event in yeast secretion. Cell *49*, 527–538.

Sloat, B. F., Adams, A., and Pringle, J. R. (1981). Roles of the CDC24 gene product in cellular morphogenesis during the *Saccharomyces cerevisiae* cell cycle. J. Cell Biol. *89*, 395–405.

Taxis, C., Maeder, C., Reber, S., Rathfelder, N., Miura, K., Greger, K., Stelzer, E. H., and Knop, M. (2006). Dynamic organization of the actin cytoskeleton during meiosis and spore formation in budding yeast. Traffic *7*, 1628–1642.

Tong, A. H. *et al*. (2004). Global mapping of the yeast genetic interaction network. Science *303*, 808–813.

Valdez-Taubas, J., and Pelham, H. (2005). Swf1-dependent palmitoylation of the SNARE Tlg1 prevents its ubiquitination and degradation. EMBO J. *24*, 2524–2532.

Van Aelst, L., and Cline, H. T. (2004). Rho GTPases and activity-dependent dendrite development. Curr. Opin. Neurobiol. *14*, 297–304.

Venable, J. H., and Coggeshall, R. (1965). A simplified lead citrate stain for use in electron microscopy. J. Cell Biol. *25*, 407–408.

Wedlich-Soldner, R., Altschuler, S., Wu, L., and Li, R. (2003). Spontaneous cell polarization through actomyosin-based delivery of the Cdc42 GTPase. Science *299*, 1231–1235.

Winzeler, E. A. *et al*. (1999). Functional characterization of the *S. cerevisiae* genome by gene deletion and parallel analysis. Science *285*, 901–906.

Wolven, A. K., Belmont, L. D., Mahoney, N. M., Almo, S. C., and Drubin, D. G. (2000). In vivo importance of actin nucleotide exchange catalyzed by profilin. J. Cell Biol. *150*, 895–904.

Wright, R. (2000). Transmission electron microscopy of yeast. Microsc. Res. Tech. *51*, 496–510.

Zajac, A., Sun, X., Zhang, J., and Guo, W. (2005). Cyclical regulation of the exocyst and cell polarity determinants for polarized cell growth. Mol. Biol. Cell *16*, 1500–1512.

Zhang, X., Bi, E., Novick, P., Du, L., Kozminski, K. G., Lipschutz, J. H., and Guo, W. (2001). Cdc42 interacts with the exocyst and regulates polarized secretion. J. Biol. Chem. *276*, 46745–46750.

Ziman, M., O'Brien, J. M., Ouellette, L. A., Church, W. R., and Johnson, D. I. (1991). Mutational analysis of *CDC42Sc*, a *Saccharomyces cerevisiae* gene that encodes a putative GTP-binding protein involved in the control of cell polarity. Mol. Cell Biol. *11*, 3537–3544.

Ziman, M., Preuss, D., Mulholland, J., O'Brien, J. M., Botstein, D., and Johnson, D. I. (1993). Subcellular localization of Cdc42p, a *Saccharomyces cerevisiae* GTP-binding protein involved in the control of cell polarity. Mol. Biol. Cell *4*, 1307–1316.